ASME Open Journal of Engineering
Online journal at:
https://asmedigitalcollection.asme.org/openengineering

Emily Porter[1]
Department of Biomedical Engineering,
McGill University,
Montréal, QC H4A 3J1, Canada
e-mail: emily.porter@mcgill.ca

Lourdes Farrugia
Physics Faculty of Science,
University of Malta,
Msida 2080, Malta
e-mail: lourdes.farrugia@um.edu.mt

Punit Prakash
Department of Electrical and Computer Engineering,
Kansas State University,
St Manhattan, KS 66506
e-mail: prakashp@ksu.edu

Raquel C. Conceição
Instituto de Biofisica e Engenharia Biomedica,
Faculdade de Ciencias,
Universidade de Lisboa,
Lisbon 1749-016, Portugal
e-mail: rcconceicao@fc.ul.pt

Devashish Shrivastava
Center for Devices and Radiological Health,
US Food and Drug Administration,
Spring, MD 20903
e-mail: devashish.shrivastava@gmail.com

Rosa Scapaticci
Institute for Electromagnetic Sensing of the Environment,
Naples 80124, Italy
e-mail: scapaticci.r@irea.cnr.it

Stefano Mandija
Department of Radiotherapy,
University Medical Center,
Utrecht 3584 CX, The Netherlands
e-mail: stefanomandija@libero.it

Marta Cavagnaro
Department of Information Engineering,
Electronics and Telecommunication,
Sapienza University of Rome,
Roma 00184, Italy
e-mail: marta.cavagnaro@uniroma1.it

Current Status and Emerging Techniques for Measuring the Dielectric Properties of Biological Tissues

The dielectric properties of biological tissues are key parameters that support the design and usability of a wide range of electromagnetic-based medical applications, including for diagnostics and therapeutics, and allow the determination of safety and health effects due to exposure to electromagnetic fields. While an extensive body of literature exists that reports on values of these properties for different tissue types under different measurement conditions, it is now evident that there are large uncertainties and inconsistencies between measurement reports. Due to varying measurement techniques, limited measurement validation strategies, and lack of metadata reporting and confounder control, reported dielectric properties suffer from a lack of repeatability and questionable accuracy. Recently, the American Society of Mechanical Engineers (ASME) Thermal Medicine Standards Committee was formed, which included a Tissue Properties working group. This effort aims to support the translation and commercialization of medical technologies, through the development of a standard lexicon and standard measurement protocols. In this work, we present initial results from the Electromagnetic Tissue Properties subgroup. Specifically, this paper reports a critical gap analysis facing the standardization pathway for the dielectric measurement of biological tissues. All established measurement techniques are examined and compared, and emerging ones are assessed. Perspectives on the importance and challenges in measurement validation, accuracy calculation, metadata collection, and reporting are also discussed. [DOI: 10.1115/1.4064746]

Keywords: Bioinstrumentation and measurements, biological systems applications, biomaterials, biomedical systems, dielectrics, electric and magnetic phenomena, standards and codes

[1]Corresponding author.
Manuscript received December 15, 2023; final manuscript received February 8, 2024; published online March 14, 2024. Assoc. Editor: Rouzbeh Amini.

Sergio Curto
Erasmus MC Cancer Institute,
University Medical Center Rotterdam,
Zuid Holland 3015 GD, The Netherlands
e-mail: s.curto@erasmusmc.nl

1 Introduction

The dielectric properties of biological tissues are parameters that characterize the way externally applied electromagnetic (EM) fields interact with the human body. These properties quantify how much of an EM field is reflected, transmitted, and absorbed by tissues. The properties are temperature- and frequency-dependent and, importantly, commonly vary with health and disease states.

Therefore, accurate measurement and understanding of dielectric properties of tissues are keys for studying the safety of exposure to electromagnetic fields, both in dosimetry studies, e.g., for assessing radiation from cell phones, Wi-Fi, etc., and in medical applications, e.g., during a magnetic resonance imaging (MRI) scan or a radio-frequency (RF) or microwave (MW) ablation treatment [1]. In particular, whether exposure is safe or not is commonly characterized by the Specific Absorption Rate (SAR) of energy absorbed into the tissues—and this energy level depends upon the values and distributions of dielectric properties of the tissues in the region [1]. Where exposures exceed safe levels, tissue heating and sensations of pain can occur, followed by tissue damage and even cell death [1].

Knowledge of these dielectric properties is also pivotal for designing and optimizing medical technologies based on transmitting EM fields into the body and/or receiving scattered field responses. Numerous technologies and clinical applications fall into this category, including but not limited to, impedance-based imaging of lungs, brain, heart, etc. [2–4]; microwave imaging or screening for breast tumors, osteoporosis, bladder volume, stroke, etc. [5–8]; and thermal therapies to treat cancer such as RF- or MW-based ablation and hyperthermia [9,10]. Specifically, the fundamental operating principles of EM technologies as medical tools are based on inherent dielectric contrasts between healthy and malignant/target tissues for various types of diseases or conditions. These systems exploit the inherent contrast between tissues to image a region, track or monitor changes over time, or therapeutically differentiate the target tissue while sparing the surrounding healthy ones.

The dielectric properties of tissues are commonly reported through the complex permittivity, ε, which is a measure of the ability of the tissue to store energy (through electric polarizability) in response to an applied external field. The complex permittivity is defined as:

$$\varepsilon(\omega) = \varepsilon_0 \cdot \varepsilon_r^*(\omega) = \varepsilon_0 \cdot (\varepsilon_r'(\omega) - j\varepsilon_r''(\omega)) \quad (1)$$

where ω is the angular frequency of the external electromagnetic field, ε_0 is the vacuum permittivity, equal to $\frac{1}{36\pi} \cdot 10^{-9} \frac{F}{m}$, ε_r^* represents the relative complex permittivity of the material, which is unitless, ε_r' is the real part of the relative complex permittivity (also called "relative permittivity"), ε_r'' is the imaginary part (which can be also expressed as an equivalent conductivity σ_{eq} as $\frac{\sigma_{eq}}{\omega\varepsilon_0}$ to easily include the static ionic conductivity σ [S/m]). We note that permeability is also a property of materials often associated with permittivity—the permeability quantifies the ability of a material to support a magnetic field. As most tissues are considered non-magnetic over most frequency ranges, we do not further consider the permeability of tissues. Instead, here, we focus on the more broadly applicable complex permittivity.

The dielectric properties of biological tissues have been reported through numerous studies and are even currently available through open-access online look-up databases. Currently, the most frequently cited database on tissue dielectric properties is provided by the Foundation for Research on Information Technologies in Society (IT'IS) [11] (>1175 citations, according to Google Scholar at the time of writing this). This database provides dielectric properties for more than 100 tissues (including from unique tissue measurements and tissues assigned properties based on the available properties of other known tissues) for frequencies spanning 10–100 GHz [12]. The source data are based primarily on the 1996 work by Gabriel et al., which represents one of the first and largest studies on dielectric properties of biological tissues comprising both literature surveys as well as measurement of *ex vivo* properties in the frequency range from 10 Hz to 20 GHz [13–15].

Since then, several groups have performed measurements of the dielectric properties of biological tissues for a variety of conditions. Despite the wide availability of dielectric data, concerns have been noted that (i) dielectric data reported is inconsistent for many tissues, and (ii) a lack of metadata reporting has made comparison and interpretation of data difficult. This is attributed to the fact that there are no standard techniques for the measurements or reporting strategies for the dielectric properties of biological tissues, and researchers or scientists generating dielectric data may each use different measurement techniques, tissue-handling procedures, and reporting protocols. Furthermore, we are aware of no proposed standards in this area.

As a result of these limitations, and similar limitations in data for other related tissue properties (e.g., thermal properties), a standards committee was initiated: the American Society of Mechanical Engineers (ASME) Thermal Medicine Standards Committee—Tissue Properties Project aims to define and standardize tissue properties and related measurement methods relevant for thermal medicine technologies. In particular, the goal is to support the evaluation of thermal effects of medical devices that produce local, regional, and/or whole-body changes in tissue temperature (i.e., heating and/or cooling), through standardization of tissue properties measurement methods and reporting criteria. Eight tissue property types are being studied under this umbrella, including "electromagnetic" tissue properties, which are the focus of this paper. The authors of this work are comprised of members of this standards committee, and span across industry, government, and academic researchers.

Therefore, our long-term objective is to propose a standard for the measurement of dielectric properties of biological tissues. However, as discussed below, our current stance is that this is a very complicated goal for many reasons—therefore, the motivation of this work is to make progress toward this goal. In this article, we review a wide array of measurement techniques used for dielectric measurement of biological tissues, both current and emerging, describing how each of them functions and assessing their benefits and limitations. We focus on techniques used in the kHz, MHz, and GHz frequency ranges, as this covers the most common medical applications that use the dielectric data of biological tissues. Above 100 GHz, into the THz range, usage of optical tissue properties (e.g., index of refraction, extinction coefficient, and absorption coefficient) becomes more common [16]. We further discuss both "direct contact" measurement techniques, i.e., those that

enable measurement of the dielectric properties of tissues with direct access to the tissue or tissue sample (including reflection and transmission-based line methods, cavity perturbation methods, open-ended coaxial probes, and electrode-based measurements), and "indirect contact" measurement techniques, i.e., those that allow in vivo, non-invasive, and non-destructive tissue measurements (e.g., electrical impedance tomography, magnetic resonance, and microwave imaging). We critically discuss the current state of these technologies and the challenges associated with identifying one technique as a potential "standard" approach. Lastly, we conclude with future work and a summary of the needs in this area.

We note that several works have reviewed or examined other informative topics related to the dielectric properties of biological tissues, including works that report reviews and/or comparisons of dielectric measurement data within and across tissue types (e.g., [13,16]); review and/or discuss measurement challenges with a single measurement technique (e.g., for open-ended coaxial probes, [17,18]); examine metadata types that can be reported for interpretable data [19]; and report on techniques for temperature-dependent dielectric studies (e.g., [20]). Complementary to these topics, in this work, we provide a critical assessment of the measurement techniques themselves.

2 Established Techniques for Measuring the Dielectric Properties of Biological Tissues

In this section, each measurement technique that is used to measure the dielectric properties of biological tissues is examined and compared. First, in Secs. 2.1–2.4, four established measurement techniques are introduced with a description of how the technique works. The limitations and advantages of each technique are detailed, and information on specific operating ranges or conditions is provided (e.g., the frequency range, broadband versus narrowband, the types of measurement samples that can be measured, destructive or non-destructive nature, temperature range, potential for in vivo versus ex vivo measurements, and so forth). Tissue types that have been measured with each technique are also noted, with references to corresponding reports from the literature. Diagrams summarizing the measurement setup for each of these techniques are provided in Figs. 1 and 2.

For each measurement technique, a search of literature works was conducted to identify tissue types that have been measured with each technique. The search engines PubMed, IEEExplore, and WebOfScience were used. The search included search terms within the title, keywords, and/or abstract.

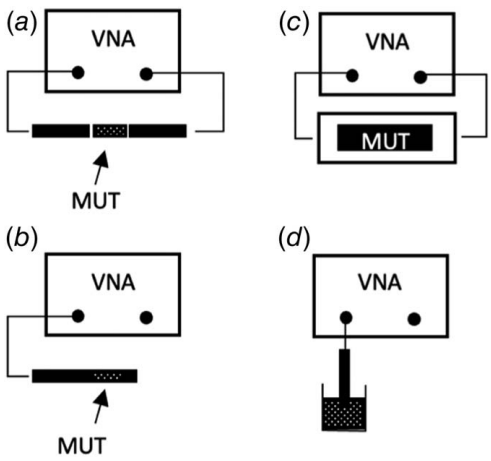

Fig. 1 Schematic diagram summarizing the dielectric measurement techniques reported in Secs. 2.1–2.3: (*a*) transmission line methods, (*b*) reflection line methods, (*c*) cavity methods, and (*d*) open-ended coaxial probe methods. VNA, vector network analyzer; MUT, material under test.

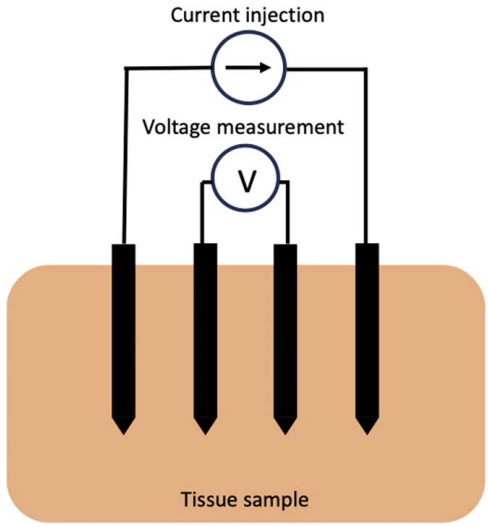

Fig. 2 The four-electrode method for dielectric property measurements involves injection of current into the tissue sample with a pair of electrodes and potential measurement across another pair of electrodes. Tissue dielectric properties are then inferred by taking into account known geometry of the electrodes and sample.

Both human and animal tissue measurements are included. Any specific search criteria applied to a given measurement technique are described within the relevant subsection below.

After the measurement techniques are described, a comparison between them is discussed in Sec. 2.5. The comparison focuses on key factors that may affect usability and convenience in measuring tissue dielectric properties.

2.1 Transmission/Reflection Line Methods. Transmission/reflection line methods involve placing the tissue sample into a section of a closed transmission line and are usually used for measuring samples with medium and high dielectric loss (loss is dependent on ε_r'') [21]. Types of transmission lines commonly used include coaxial lines (circular cross section) and waveguides (often with rectangular cross sections). Typically, each side of the line is connected to one port of a network analyzer, and the two-port S-parameters are measured: the reflection coefficient, S_{11}, and the transmission coefficient S_{21} [17,22–24]. Using this configuration, both the permittivity and permeability of the material can be determined. In a similar yet alternate approach, the line may be terminated in a short and only the one-port reflection coefficient is measured (commonly known as the Roberts and von Hippel technique or the Short-circuit line method) [25–27]. From the S-parameters, the complex permittivity (and complex permeability) can then be obtained using conversion algorithms [28–32].

Waveguides and enclosed coaxial lines can be used to measure the properties of various types of tissues, including biological fluids, semi-solid soft tissues, and solid tissues. However, the sample must either fill the fixture fully, with ideally no air gaps, or waveguide or coaxial gap correction should be implemented [21,24]. To this end, the faces of the tissue sample should be smooth and even, and placed perpendicular to the incoming signal. Due to these requirements, it may be challenging to achieve a high-quality measurement with semi-solid or solid tissues. Additionally, as this method requires cutting or machining the sample into a specific shape and size, only *ex vivo* measurements can be conducted. Moreover, this method has limited accuracy when the sample length is multiple of one-half wavelength of the material [33]. The conversion algorithms also typically assume that the sample under test is homogeneous. With transmission line methods, both reflection and transmission measurements can

be conducted over a broad frequency range (spanning MHz and GHz ranges [23,26]); however, different waveguides may need to be used for different segments of the range [34]. The possible frequency range of measurements is limited by the practical size of the sample (at low frequencies, the sample volume required may be impractically large for tissues, and at high frequencies, the sample volume required may be impractically small) [23,26,27]. Measurements can be obtained at different temperatures by immersing the line (if watertight) in heated water or a heated environment, with a wide range of temperatures possible (measurements spanned from 20 °C to 100 °C) [34]. Temperature control may be easier to achieve in waveguides than coaxial lines, since in coaxial lines the inner conductor is internal to the structure, away from the temperature-control source [27]. Both isotropic and anisotropic materials can be measured using waveguides [23]. Using network analyzers to record the S-parameters can lead to low uncertainties in the resulting permittivity, e.g., $< \pm 1\%$ at microwave frequencies for liquids [27].

As the number of works using this measurement technique is limited, a comprehensive search was readily possible. A search for studies reporting tissue dielectric property measurements obtained with the transmission/reflection line measurement technique was performed using the search strategy: (any of category1) and (any of category2) and (any of category3), where category1 = {dielectric properties, dielectric measurement, dielectric spectroscopy, dielectric characterization, dielectric characterization, permittivity, permittivities, dielectric constant, dielectric constants}, category2 = {waveguide, transmission line, short-circuit line, short-circuit line}, and category3 = {tissue, tissues, biological, bio, human, animal, organ}. Note that reports using the open-ended coaxial line are not included here and will be discussed in Sec. 2.3. The resulting search results indicate that studies have reported measurements using transmission/reflection line techniques that involve a number of various tissues (liquid, soft, and hard), including brain tissues [22,26,35,36], bone [34], liver [35,37–39], lung [37], kidney [37,39], muscle [35,37,39–41], fat [35,40,41], skin [38], pancreas [37], spleen [35,39], stomach [39], intestine [39], heart [39], tumorous tissues [35], blood [42–46], and blood cells [47].

2.2 Cavity Perturbation. Cavity perturbation methods, also called cavity resonance methods, involve placing the tissue sample within a cavity that is known to have a given resonant frequency. The dielectric properties of the sample are quantified by measuring the resonant frequency and quality factor ("Q-factor") when the sample is placed in the cavity, often as compared to an empty cavity (typically measured through transmission parameters with the cavity connected to a Vector Network Analyzer—VNA) [17,23,27,48,49]. Using these two parameters, the complex permittivity (and permeability) of the sample can then be calculated at the resonant frequency [23,49]. The dielectric properties are a result of averaging of local dielectric properties across the sample volume [49]. The derivation for obtaining the complex permittivity based on the resonant frequency and Q-factor data can be found in Ref. [50]; however today software, often built-in to a VNA, can achieve this conversion [23,51].

While individual dielectric measurements can be done typically only at a single frequency [17,23,49], measurements can be performed at various frequencies through the use of cavities with different dimensions [49]. Commonly, frequencies from about the mid-hundreds of MHz to mid-tens of GHz ranges are convenient for measuring the properties of biological tissues [23,49,51–56]. The method is generally useful for small tissue samples [23,48] (e.g., volume of 10 mm^3 in Ref. [50]), which can be useful for measuring the properties of tissues as some excised samples can be quite small. A detailed analysis of sample size, related to cavity shape and properties of the material under test, was provided in Ref. [48]. Due to the sample being required to fill the cavity, achieving accurate measurements with soft and hard tissues may present challenges. For example, an excised tissue sample to be cut or pressed into the required shape and size could lead to a loss in tissue fluid, and uneven edges could lead to air bubbles or gaps between the sample and the cavity, both of which would affect the dielectric measurement [23,49]. As the cavity method requires sample shaping, in-vivo measurements are not feasible.

As the number of works using this measurement technique is limited, a comprehensive search of tissues measured was possible: a search for works reporting tissue dielectric property measurements obtained with this measurement technique was performed using the search strategy: (any of category1) and (any of category2) and (any of category3), where category1 = {dielectric properties, dielectric measurement, dielectric spectroscopy, dielectric characterization, dielectric characterization, permittivity, permittivities, dielectric constant, dielectric constants}, category2 = {cavity, cavities}, and category3 = {tissue, tissues, biological, bio, human, animal, organ}. The resulting search indicated that various types of tissues, including soft tissues and biological fluids, have been measured using the cavity perturbation technique. Specifically, studies have reported measurements on samples of urine [56–59], blood [60,61], breast tissues [52,62], fat [53,63], liver [53,63], marrow [53,63], cerebrospinal fluid [55], bile [64], bile stones [64], gastric fluids [64], saliva [64], nerve tissue [65], cancer cells [54], and other cell suspensions [66].

2.3 Open-Ended Coaxial Probe. The open-ended coaxial probe technique is a wideband technique suited for performing non-invasive measurements of the dielectric properties of a material with little manipulation. The technique is based on the measurement, by a VNA, of the complex reflection coefficient of a coaxial cable, the open end of which is placed in contact with or slightly inserted into the material under test (MUT). In correspondence to the discontinuity between the coaxial cable and the MUT, the fundamental mode (transverse electromagnetic—TEM) which propagates inside the coaxial cable is partially radiated into the MUT and partially reflected, giving rise in the input line to a reflected TEM mode and to evanescent higher-order transverse magnetic (TM_{0n}, $n = 1,2, \ldots$) modes [67]. The VNA measures the complex reflection coefficient, which is directly linked to the complex permittivity of the MUT. Several papers extensively described the models that could be used to derive the dielectric properties of the MUT from the measured reflection coefficient. Some works [67–69]) developed precise models based on rigorous electromagnetic solutions. These methods are usually referred to as integral methods. They allow for achieving high accuracy in the results at the price of high mathematical complexity and high computational cost. A simpler analysis is achieved by representing the open-end of the probe in contact with the MUT with a lumped element circuit [70–73]. The circuit has been implemented in several ways, with different levels of complexity. The simplest implementation foresees only the presence of capacitances to represent the electromagnetic field stored in correspondence to the cable aperture (e.g., [70]). In more complex implementations, the radiation resistance is included to represent the electromagnetic field radiated into the MUT [71]. To characterize the circuital elements, before measuring the MUT, a calibration procedure is needed, consisting of the measurement of the complex reflection coefficient in three or four—according to the adopted circuit—known loads, usually made by open, short and one or two liquids whose dielectric properties are well-known, e.g., distilled water [74–76].

As stated before, the open-ended probe technique has a very simple and straightforward experimental arrangement and procedure. However, the models adopted to represent the discontinuity between the open-ended coaxial probe and the MUT are usually based on the hypotheses that the MUT is homogeneous and of infinite thickness, and its transversal dimensions are such to completely confine the electromagnetic field [70,77]. To help this latter confinement, some coaxial probes are equipped with flanges around the open end of the coaxial cable. Moreover, the homogeneous sensing volume is probe-dependent, and also depends on the

frequency and tissue dielectric properties [78–83], which can make it difficult to assess on a general basis the minimum tissue region required. The measurement is also sensitive to the pressure of the probe–sample contact [84].

The frequency band in which the open-ended coaxial probe technique can be used depends on the model used to reconstruct the MUT dielectric properties as well as on the used probe [85,86]. As an example, when the lumped element circuit is used, if only capacitive elements are included in the model, then the technique applicability is limited up to frequencies of a few GHz [70]. Higher frequencies, in fact, need the modeling of the radiation into the MUT, i.e., the insertion of the radiation resistance. When this resistance is introduced, the maximum frequency of application can be increased up to tens of GHz [85,87]. Higher frequencies require more accurate integral models. With reference to the low-frequency limit, this is dictated by the sensitivity of the reflection coefficient to changes in the MUT dielectric properties. In particular, the higher the dielectric properties, the lower the sensitivity of the reflection coefficient [88]. Since biological tissues assume high dielectric properties at low frequencies, the technique loses sensitivity for decreasing frequencies. In general, the open probe technique is applied starting from about 200 MHz [89], even though measurements are possible up to about 10 MHz [86,90]. At even lower frequencies, the effect of polarization impedance appearing at the interface between electrodes and biological tissues becomes the most significant source of error in the reconstruction of the MUT dielectric properties [14].

The number of studies reporting the dielectric properties of biological tissues measured with this technique is very numerous (initial searches found several hundred hits) and therefore we do not attempt to systematically list all of them here (indeed, to do justice to such a summary would require its own full paper). Instead, we present examples that represent the various types of tissues and measurement scenarios under which measurements with the open-ended coaxial probe have been conducted. In one of the most comprehensive and commonly referenced reports to date, Gabriel et al. reported measurements with the open probe technique described here across the frequency range of 130–20 GHz, spanning *in vivo* (human skin and tongue) and in vitro measurements on human and animal tissues, with properties measured for a total of 16 soft tissues and 1 hard tissue [14]. This measurement study provided the basis for the IT'IS foundation's database of tissue dielectric properties, which is currently the most referred-to database of dielectric properties of biological tissues [11]. Since the work of Gabriel in 1996, numerous studies, measuring tissues using the open-ended coaxial probe, have been reported, including biological fluids (e.g., blood [91–94], urine [95,96]), soft tissues (e.g., breast [97–99], liver [100], etc.), and hard tissues (e.g., bone [101–103]). Most tissue measurements have been performed ex vivo [97,100]; however, indeed, some have been conducted *in vivo* [104–106].

2.4 Impedance-Based Methods. At frequencies up to a few MHz, tissue can be measured with a four-electrode approach. This technique employs four electrodes, typically arranged in a linear configuration, in contact with the tissue under test. The two outer electrodes are used to inject a known alternating current into the tissue sample, the potential difference across the two inner electrodes (the "sensing electrodes") is recorded, and the ratio of the voltage to the current is the tissue impedance. The impedance, Z,

$$Z = R + jX \tag{2}$$

includes resistive (R) and reactive (X) components, and is a function of the frequency of the applied current, tissue conductivity (σ), tissue relative permittivity (ε_r'), and the geometry of the electrode/tissue interface. Tissue conductivity and relative permittivity can be related to the complex impedance as a function of a geometry factor. For idealized electrode geometries, the geometry factor can be determined analytically; alternatively, the geometry factor can be determined by taking calibration measurements on samples of known dielectric properties (e.g., deionized water) [107].

An amplifier with a very high input impedance (~GΩ) should be used to measure potential across the sensing electrodes. In principle, a pair of electrodes can be used for both current injection and voltage measurement, however, such a measurement is prone to errors due to electrode polarization. Electrodes comprised of inert materials (e.g., Pt, Au) with high electrical conductivity are typically employed [108]. Measurement systems employ a range of different electrode geometries/form factors, such as flat, disc-shaped electrodes for surface measurements [109], needle-type electrodes that can be inserted/immersed into the sample [110], and electrodes printed onto flexible substrates [111]. Care should be taken to determine the geometry factor under measurement conditions emulating the eventual use case. For example, with needle-type electrodes that are inserted into the sample under test, the geometry factor is typically a function of the electrode insertion depth [112]. This approach can be extended to an array of electrodes in contact with tissue and multiplexing across the electrodes applying current and measuring voltage; the resultant measurements can be analyzed to estimate a map of the underlying tissue dielectric properties, which forms the basis of electrical impedance tomography [113].

As with the open-ended coaxial probe method, the four-electrode approach has been widely used and resulting measurements of the electrical conductivity are available for a wide range of normal and pathologic animal and human tissue. Rather than attempting to provide an exhaustive review of this expansive body of literature, we present examples of scenarios in which the four-electrode method has been employed for tissue dielectric property measurements. Conductivity data using needle-type electrodes have been reported for *in vivo* and *ex vivo* measurement of tissue, including prostate gland, brain, liver [110,114,115], myocardium [116], blood [117], and kidney [118]. This technique has also been incorporated into an apparatus for measurements of conductivity as a function of temperature [119], with application to monitoring changes in tissue state during thermal interventions.

2.5 Comparison of Established Measurement Techniques. Table 1 provides a summary comparison of the four established dielectric measurement techniques. The techniques are compared across several features of interest, including the ability to perform *in vivo* measurements, whether the measurement is non-destructive, the frequency range, and the samples able to be measured. Whether or not commercial off-the-shelf measurement options are readily available is also indicated.

3 Emerging Dielectric Measurement Techniques

In this section, emerging measurement techniques for estimating the dielectric properties of tissues are highlighted. These techniques include both direct contact (Sec. 3.1) and indirect contact methods (Secs. 3.2–3.4).

3.1 Open-Ended Coaxial Probe-Based Transmission Measurements. Meaney et al. [120] developed a transmission-based method for dielectric properties measurement, in the 2 to 6 GHz frequency band. A schematic of the setup is shown in Fig. 3, where two open-ended coaxial probes are immersed inside the material under test (MUT), facing each other. The probes work as two "low-efficiency antennas," and the measured transmission coefficient (S_{21}) is used to analytically solve the complex permittivity of the MUT as detailed in Ref. [120]. The method is suitable for the characterization of heterogeneous samples, as the sensing depth is approximately 1.5 to 2 cm, which is considerably larger than the one of the traditional (reflection-based) Open-Ended Coaxial Probe (OECP) (fractions of a millimeter [121]). The measurement results in an estimation of the bulk or average properties across the

Table 1 Comparison of established dielectric measurement techniques. (Y = Yes; N = No)

	Transmission line (waveguide) methods	Cavity methods	Open-ended coaxial probe	Impedance-based methods
In vivo measurements	N	N	Y	Y
Non-destructive measurements	N	N	Y	Y
Frequency band(s)	MHz–GHz	MHz–GHz	10 MHz–50 GHz	kHz–~ few MHz
Broadband or narrow band	Broadband (using different guides)	Narrowband	Broadband	Broadband
Types of samples	Semi-solids, hard	Liquids, semi-solids, hard	Semi-solid, liquids	Solid, semi-solids, liquids
Sample size/dimensions	Related to dimensions of waveguide	Related to dimensions of cavity	Related to the dimension of the probe	Dimensions and number of electrodes determine spatial resolution
Commercially available	Y	Y	Y	Y

heterogeneous sample. The application is best suited for liquid or semi-solid samples as the reconstruction formula entails measuring the S_{21} at several separation distances; but it can be extended to solid MUT, if one can accept handling and potentially damaging the sample. Meaney et al. validated the method on a trabecular portion of a bovine bone, retrieving dielectric properties in line with those reported in the literature [122] for the same tissue.

A second transmission-based OECP for dielectric measurement (2- to 6-GHz frequency band) was proposed in Ref. [123]. The setup is the same as the one described above [120], while the de-embedding of dielectric properties relies on the empirical comparison between experiments and simulations. The method is based on the hypothesis that an accurate representation of the experiments in simulation should give approximately the same output (same S_{21}) of the actual experiments. The method is suited for relatively small size (a few millimeters) heterogeneous samples, where (i) the electromagnetic-field reflections at the MUT-air interface are not negligible as assumed in Ref. [120], and (ii) sample puncturing is not possible. Even though the method in Ref. [118] was originally thought for excised lymph node dielectric measurement, the authors report that this was only tested on regular-size (cuboid) phantoms, showing preliminary promising results.

3.2 Electrical Impedance Tomography. Electrical impedance tomography (EIT) is an imaging technique built upon the impedance-based measurement methods discussed in Sec. 2.4. EIT employs multiple electrodes placed across the tissue regions of interest, as shown in Fig. 4, and aims to generate a map of the estimated tissue electrical properties (i.e., conductivity) from potential measurements across several combinations of electrode pairs. The measured voltages $\mathbf{V}$ are related to the conductivity distribution $\boldsymbol{\sigma}$ by:

$$\mathbf{A}\boldsymbol{\sigma} = \mathbf{V} \tag{3}$$

where $\mathbf{A}$ is referred to as the sensitivity matrix. Determining the conductivity distribution $\boldsymbol{\sigma}$ of the tissue regions requires a solution to the above ill-posed, ill-conditioned inverse problem. Due to the measurement approach involving injected currents, the relative permittivity is not typically a parameter that is measured.

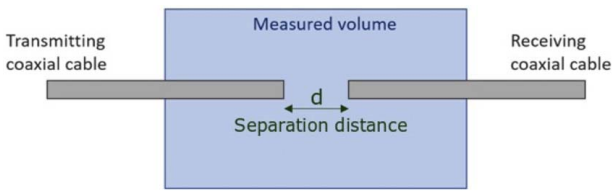

Fig. 3 Schematic representation of Meaney et al.'s [120] transmission-based Open-Ended Coaxial Probe (OECP) for dielectric measurements. Two OECP (transmitting and receiving) are immersed inside the Material Under Test and placed in the same direction, facing each other.

Numerical models play a central role in the solution of the inverse problem. These models solve the quasi-static electric field equation to predict the voltages at the measurement electrodes for a specified conductivity map. Using such models, both direct and iterative methods have been applied to solve for the conductivity distribution.

EIT systems have been designed for operation at frequencies from ~10 kHz to a few MHz [124]. Systems have been developed using a variety of form factors, ranging from electrodes placed externally on the skin surface [125], incorporated within devices placed within body lumens/cavities [126], or integrated within minimally-invasive needles/catheters [127] with each placing constraints on the number of electrodes. A key strength of EIT is that it enables estimation of tissue conductivities (or resistivities) without necessarily requiring direct contact with the tissue of interest. As an imaging modality, although EIT suffers from poor spatial resolution, it offers the advantage of using non-ionizing energy, can be made relatively portable, and has excellent temporal resolution [124]. While EIT is well suited to measuring changes in conductivity of a region, or contrast in conductivities properties between two regions, it is perhaps less well suited to yielding absolute estimates of electrical conductivity.

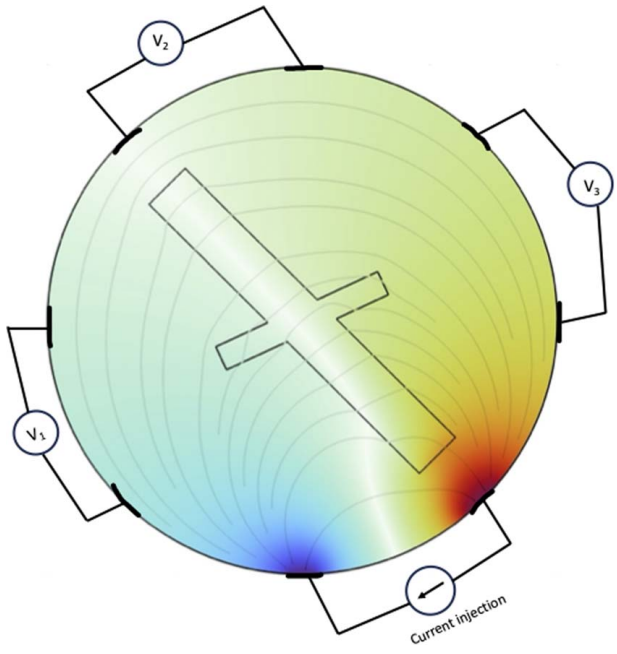

Fig. 4 Electrical impedance tomography offers a means for non-invasive estimation of tissue electrical property maps. Current is injected between a pair of electrodes, and potential measurements (V_1, V_2, and V_3) between other electrodes are gathered. An inverse modeling approach is applied to estimate electrical property maps from the measured data.

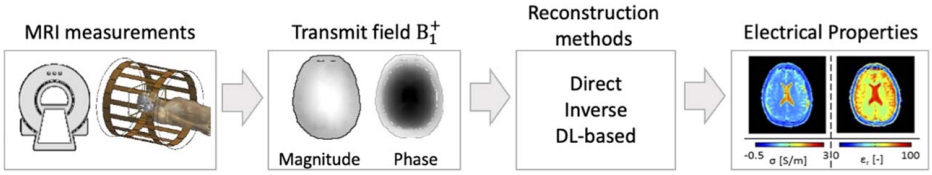

Fig. 5 Flowchart of work for the extraction and estimation of dielectric properties from MRI images

EIT systems have been investigated for a range of indications where changes in conductivity relative to a baseline case can be used to inform clinical decision-making. These include stroke detection and classification [128,129], bladder volume assessment [130,131], and lung ventilation and perfusion [132,133]. EIT has also been applied for the detection and classification of tumors, or guiding treatment, in sites including the prostate [107,134], breast [135], and the oral cavity [136].

3.3 Extraction of Dielectric Properties From Magnetic Resonance Images: Electrical Properties Tomography. Electrical Properties Tomography (EPT) is a magnetic resonance (MR)-based technique that aims at measuring tissue conductivity and permittivity noninvasively (Fig. 5). These properties are derived at Larmor's frequencies (64–300 MHz) using standard MR systems and MR sequences. This technique exploits the fact that the dielectric properties of tissue distort the MRI radiofrequency transmit field, known as the B1+ field, which is used for spin excitation. In MRI, it is possible to measure this distorted B1+ field with standard imaging techniques. From these measurements, tissue dielectric properties are therefore derived [137–139]. Since Maxwell equations relate local electric fields to local magnetic field—and not part of the magnetic field such as B1+, assumptions are made regarding the missing part of the magnetic field (i.e., B1-) to estimate dielectric properties. The accuracy of the estimation depends on the accuracy of the assumption. Physics-based EPT reconstructions rely on the Helmholtz equation written in terms of the transmit radiofrequency MR field and assuming negligible magnetic permeability variations. In this equation, the complex wave number includes the tissue dielectric properties. With few assumptions on the measured field, to a leading order for low MRI field strengths (64–128 MHz) the permittivity is proportional to the magnitude of the B1+ field, while the conductivity is proportional to the phase of the B1+ field.

Nowadays, there are several reconstruction approaches used to extract these properties from the measured MRI field [140–157]. Following the Helmholtz model, direct methods extract the dielectric properties from the measured B1+ field locally by computing spatial derivatives of the measured field. These methods allow fast retrieval of the underlying properties. However, they suffer from noise amplification caused by the computation of local spatial derivatives and errors at boundaries between tissues. Yet, mitigation strategies like imaging filters and the exploitation of available MRI magnitude images to compute spatial derivatives have been proven to increase the quality of the reconstructed images. Alternatively, to avoid the computation of spatial derivatives of measured B1+ fields, inverse methods have been proposed. These methods iteratively minimize the discrepancy between the measured B1+ field and the B1+ field resulting from an initial guess of the dielectric properties distributions. Because spatial derivatives are not computed, these methods are intrinsically noise-robust and allow for better reconstructions at tissue boundaries. Yet, they are more computationally demanding with respect to direct methods. Additionally, to avoid overfitting, regularization strategies are commonly employed.

Finally, following the great success of artificial intelligence (AI) for image analysis and reconstructions, first attempts at using deep learning for dielectric properties reconstructions have been proposed. Feed-forward deep learning strategies offer great potential in terms of noise robustness, computational speed, and input images. Yet, generalization to structures not seen during the training phase might be an issue [158–161]. To overcome this issue, deep learning may be combined with data-driven approaches where deep learning can be used as the initial guess of inverse, physics-based reconstructions, thus leading to better and faster convergence, or it can be used for denoising purposes for direct physics-based reconstructions, thus leading to less noise amplification and fewer errors at tissue boundaries [162]. Ultimately, physics-informed, iterative networks can also be used, where the physics is included in the network by a forward operator linking the dielectric properties to the measured B1+ field. These networks may overcome the computational burden of iterative reconstructions while including a priori information, maintaining the physics, and imposing data consistency.

Early *in vivo* evidence of conductivity reconstruction with healthy and pathologic tissues has been presented recently, demonstrating the potential of this methodology to differentiate between healthy, benign, and malignant tissues. In brain tissue, a positive correlation between tumor grade and an increase in tissue conductivity was observed. The measured conductivity in the pathologic tissue was much higher compared to normal parenchyma [163], while brain tissue conductivity among healthy subjects does not show significant variations [164]. In addition, it was recently observed in rat tumor models that tumor conductivity measured at 401 MHz increased over time while mean diffusivity obtained from diffusion MRI measurements did not change [165]. These preliminary results suggest that conductivity values at MHz frequencies can provide complementary information about the tumor microenvironment with respect to mean diffusivity.

In breast tissue, it was observed that a conductivity increase in the tumor (for tumors larger than 2 cm) is correlated to the mitotic score [166]. The mitotic score is an index for cell proliferation and a high score is related to poor prognosis. It is therefore hypothesized that cancer cells with increased mitosis have lower membrane potentials and thus higher negative surface charges on their membrane, and so they tend to have an increased ability to absorb positive ions. This active movement of ions might increase tissue conductivity. In other studies, not only the increase in tissue conductivity in the tumor tissue was confirmed but also it was demonstrated the ability of conductivity imaging to differentiate benign and malignant lesions [167,168]. As for brain tissue, a comparison between conductivity and diffusion MRI has also been performed for breast tissue. Preliminary *in vivo* data on breast cancer patients show that conductivity and the apparent diffusion coefficient are negatively correlated [169]. In tumor tissues, the high cellularity or cellular swelling leads to lower diffusion coefficients, while the conductivity increase arises from differences in water content and ionic concentration. However, this correlation was not found to be significant in the presence of necrosis.

Conductivity imaging was also applied to cervical cancer at 128 MHz. It was observed that the average conductivity measured *in vivo* in 10 patients was 13% higher than *ex vivo* literature values. This has therefore been shown to have a substantial impact on cervical tumor temperatures achieved during hyperthermia [170], where the higher conductivity in the bladder and the muscle tissue surrounding the tumor leads to higher power dissipation, and therefore to lower tumor temperatures [171].

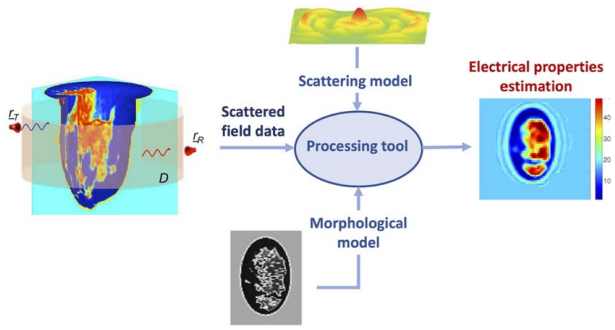

Fig. 6 Schematic representation for estimating electrical properties through microwave imaging measurements

The impact of tissue conductivity on the temperature increases in tissue when these are exposed to radiofrequency fields may be relevant not only for treatment planning but also for safety aspects. It has been shown that conductivity variations may not lead to substantial variation in global Specific Absorption Rate (SAR) but could be relevant for local SAR, especially at high fields where multi-transmit arrays are used. This information can be used for pulse sequence design and optimization [137,172,173].

While *in vivo* tissue conductivity measurements with MRI are becoming more and more available, tissue permittivity reconstructions with EPT at clinical MRI frequencies are severely affected by noise. Only in a few studies at high field strengths are permittivity reconstructions shown. In a first study at 300 MHz, it was observed that the permittivity values of white and gray matter in vivo are higher than the ones reported from *ex vivo* measurements [174]. In another study at 401 MHz in rat tumor models, the authors showed the capability of conductivity as well as permittivity maps to discriminate regions within tumors [145,175]. Additionally, as the processing of MRI data to estimate the complex permittivity is conducted at the MRI scanner frequency, reliable and validated dispersion models must be developed if the use of these properties is desired over a broader frequency band.

3.4 Microwave Imaging for Tissue Dielectric Properties Estimation. The physical phenomenon underlying microwave imaging (MWI) is the electromagnetic scattering that occurs when an electromagnetic field in the range of microwave frequencies interacts with an object, inducing an electromagnetic current. Such an induced current acts as a source that irradiates an electromagnetic field (known as a scattered field), whose properties depend on the morphological and electromagnetic properties of the object that generated it. From this phenomenon follows the possibility of retrieving the features (both electromagnetic and morphological) of the scenario under investigation, in a non-invasive way, through the measurement and the processing of electromagnetic fields (Fig. 6).

MWI is an appealing option for estimating the dielectric properties of tissues for several reasons from different points of view. First, it is non-invasive, since the relevant "sensors" are antennas positioned outside the region of interest (and outside the human body). It is based on low-cost technologies, if compared to MRI or CT equipment. Finally, it can provide tissue characterization at the needed frequencies of interest, based on the application one is aimed at (treatment plan for electromagnetic therapies, dosimetry, etc.). However, it must be said that the characterization of a region of interest via MWI requires the solution of an inverse electromagnetic scattering problem, which is non-linear and ill-posed, hence highly prone to false solutions if not properly handled [176,177]. Additionally, as compared to MRI and CT, MWI exhibits a low spatial resolution, which would ultimately impair the goal of building reliable computational models. To overcome this issue, recent works suggested the incorporation of high-resolution morphological information from MRI or CT into the MWI algorithms [178–183]. The segmented medical images are used as a patient-specific basis of the unknown electric properties, allowing a dramatic reduction of the unknown parameters to retrieve, with a crucial effect on the reliability and accuracy of the solution of the inverse scattering problem [184]. Such an approach has been also suggested and validated to work with only amplitude data [179], with a positive effect on the required measurement time and accuracy, being the phase measure largely affected by uncertainties.

To date, the majority of works concerning the possibility of retrieving quantitative information on tissues' electric properties via MWI are at a very preliminary stage, involving numerical validations on realistic phantoms [185–188], or very simple experimental tests in laboratory conditions [189–192]. However, there are also some relevant examples of first experimental tests on volunteers, which are worthy of mention [193–196].

3.5 Summary and Discussion. A summary comparing the emerging approaches for dielectric measurements of biological tissues is provided in Table 2. For ease of comparison across approaches, the table covers the same key features of measurement techniques as that in the existing measurement technique summary of Table 1.

Three of the four emerging approaches (i.e., electrical impedance tomography, and microwave imaging) offer non-invasive imaging of the body, as an opportunity to achieve patient-specific dielectric properties of wide regions of the body, under in vivo conditions. This potential for non-invasive dielectric characterization of human tissues and the human body is highly attractive. Besides

Table 2 Comparison of emerging dielectric measurement techniques

	OECP Transmission measurements	Electrical impedance tomography	Electrical properties tomography	Microwave imaging
In vivo measurements	Y	Y	Y	Y
Non-destructive measurements	Y	Y	Y	Y
Frequency band(s)	MHz—GHz	kHz—MHz	MHz	MHz—GHz
Broadband or narrow band	Broadband	Broadband[b]	Narrowband	Broadband
Types of samples	Any (solid[a], liquid, semi-solid)	Any (solid, liquid, semi-solid)	Any (solid, liquid, semi-solid)	Any (solid, liquid, semi-solid)
Sample size/dimensions	Related to dimensions of OECP	Related to size and spacing of electrodes		Related to size and spacing of antennas
Commercially available	N	Y	N	N

Note: Y, Yes; N, No.
[a]Solid samples may present additional measurement challenges (Sec. 3.1).
[b]Measurements at single or multiple frequencies possible.

the well-known discrepancies between ex vivo and in vivo characterization [104,197–199], patient-specific tissue properties could also be specifically characterized for each individual patient, overcoming uncertainties due to the natural variability of tissue electric properties between humans [14,200]. In addition, the straightforward direct and invasive measure of the in vivo properties is not always feasible for all tissues, e.g., bone and bone marrow [201] and, even when possible, it only provides local information at a single time instance, leading to reporting of average inter-patient values and limiting data on inherent variability in property values [200].

4 Discussion: Toward a Standard

4.1 An Ideal Measurement Technique? As evidenced by the numerous tissue measurements that have been conducted with the techniques reported in Secs. 2 and 3, there are several well-established dielectric measurement techniques that can be suitable for measuring the dielectric properties of tissues. The technique of choice for any given measurement may vary based on the application and the need, for example, whether the measurement needs to take place in vivo or ex vivo, the tissue sample size and form, the desired frequency range, and so forth. We note that there is no single measurement technique that can be used across all relevant scenarios.

This leads to the question of whether there is the best measurement technique given a specific scenario (e.g., measuring the dielectric properties of a freshly excised $0.5 \times 2.0\ \text{cm}^2$ bladder wall sample at 60 °C, at 300 MHz). While the advantages and limitations of each of the above-mentioned measurement techniques can be assessed for this scenario, it is in general very challenging to quantitatively compare techniques with the information available in the literature at this time. This is attributed to the fact that tissues are not straightforward to work with and many confounders affect the resulting data, and different works contain different strategies for measuring, defining, and reporting accuracy and repeatability. Confounders may include, but are not limited to, tissue measurements conducted ex vivo versus in vivo, time from excision, temperature, dehydration, tissue handling and processing, and so forth. It has proven difficult to examine the effects of only one confounder while holding all others fixed, and we are not aware of studies that have been able to compare the impacts of various confounders across different measurement techniques. In a recent publication [18], the current state and open challenges on the topic of key dielectric measurement confounders have been summarized.

Overall evaluation of uncertainty when measuring tissues is not necessarily trivial—many contributions to the uncertainty may be present and the contributions may be different according to the measurement technique used and the sample handling procedures. Furthermore, accuracy is application dependent—e.g., in general, measurements with a commercial open-ended coaxial probe may be achievable with an accuracy of, e.g., ±5 or ±10%, depending on the probe size [202]; however, these values are not indicative of the accuracy of measurements on tissues specifically. Therefore, future work in this area may benefit from comparing techniques through measurements of the same tissue samples, to gather further information about which measurement technique(s) may be most suitable for different tissues or different measurement scenarios.

Based on such comparisons, in the future, a standard measurement technique for dielectric measurements of tissues could perhaps be identified (for dielectric measurements of tissues within a specific set of scenarios, as mentioned earlier). It may be argued that an ideal measurement technique would be the one that can be used to meet as many measurement requirements as possible, e.g., enables measurements across broad frequency ranges; broad temperature ranges; on *in vivo* and *ex vivo* samples; on liquid, soft, and hard tissues; small and large volume samples; with low-cost off-the-shelf measurement equipment available that is easy and fast to use reliably. However, it must be considered that achieving most of the considered requirements could not necessarily lead to the most accurate technique. Additionally, as already cited, according to the application for which measurements are taken, different aspects can assume importance, e.g., resolution at high frequencies, versus temperature dependence for thermal applications, and so on. In any case, whichever technique would be considered, it should include the ability to perform validation measurements and calculate and report accuracy in a meaningful, consistent manner. Finally, a strategy for reporting metadata is vital to the possibility of sharing measurement results and encouraging repeatable measurement studies. Therefore, while it is challenging to identify a single ideal method for dielectric property measurements, standardizing reporting criteria is anticipated to contribute to the generalizability of reported measurements, their interpretation, and their use.

4.2 Measurement Validation and Accuracy. For any technique that is selected for dielectric measurements of tissues, it is preferred that validation with a known standard material (i.e., a material with known, traceable dielectric properties over the frequency range of interest) is achievable, and the accuracy of this measurement is quantified. This enables confidence in the measurement result and comparison of measurement results achieved in different setups and across labs.

Commonly, liquids are used for validation measurements, e.g., saline solutions or alcohols, as they are well characterized across wide frequency bands and temperature ranges, and readily available and easy to obtain [17,203,204]. However, the properties of liquids used may not fully encompass the range of dielectric properties of tissues, and therefore, the accuracy values may not be representative of measurements on materials with those properties. Furthermore, dielectric measurements with liquids rarely introduce the same amount or sources of uncertainty as measurements on actual tissue samples would—so, while measurements on liquids can indicate the functionality of the measurement system itself, they do not necessarily provide strong insight into the accuracy of using the measurement system to measure dielectric properties of solid/semi-solid tissues.

To this end, it may be valuable in the future to develop a set of standard test objects (tissue-mimicking "phantoms"), which model tissues in terms of the expected dielectric property values, structure, and mechanical properties. Some proposed standard phantoms have been developed for tissue property measurement applications already (e.g., for electrical properties tomography [205,206]). In the broader context of dielectric phantoms, such a set could include a series of phantoms that encapsulate different dielectric property values, range from soft semi-solid to hard phantoms, and include homogenous and heterogeneous designs. Well-characterized standard test phantoms would enable the measurement and characterization of accuracy on tissue-like materials and may provide accuracy values that are more representative of those experienced with actual tissue samples. However, adding to the challenge of developing phantoms to test measurement accuracy is that different system setups may require different phantom shapes/sizes, so the same phantoms may not be usable across dielectric measurement set-ups. Additionally, such a diverse array of phantoms would need to be long-lasting and shelf-stable to enable long-term repeated measurements, which currently presents non-trivial technical challenges. Moreover, phantoms are unlikely to be able to fully incorporate all tissue-related measurement effects, such as dehydration and seepage during measurements, which is why reporting the measurement metadata is also a key component of achieving consistent and reliable dielectric data.

4.3 Metadata and Reporting. The reporting of metadata alongside the measured data is extremely important: it enables re-use of the data, comparison of data from different sources, and simplifies interpretation of the measurements. To this end, data should be reported following the FAIR (Findability, Accessibility, Interoperability, and Reusability) principles [207]. This should include

publishing all data and important metadata related to the measurement, including the material that was used for validation, the equations used for quantifying the accuracy, and the calculated accuracy of the measurement.

Reporting additional metadata beyond the measurement validation is also important—and having standard methods for reporting this data—including what types of data to report, is highly useful. One way of achieving this is through minimum information models, i.e., minimum information checklists for collecting and reporting metadata. These have been used in other fields as a strategy for increasing the reproducibility of studies through use of a standard guide. For example, the Minimum Information About a Microarray Experiment (MIAME) guideline, published in 2001, has become the standard requirement for publishing papers and repositories in the field of microarray-based studies [208]. To this end, the MINDER (minimum information for dielectric measurements of biological tissues) framework was proposed in 2017 [19], however, it has not yet reached widespread usage.

A very significant challenge here is the lack of consensus as to what types of metadata are "important" enough to report. In tissue measurements, there can be a very large number of parameters that may impact the properties—spanning from the animal source (e.g., age, sex, condition, anesthesia, etc.), to the tissue-handling protocols (e.g., how the tissue was excised, stored, transported), to the treatment of the tissue during measurement (e.g., held at a warmed temperature, hydrated with saline solution, dabbed dry with tissues, etc.), to the measurement procedure itself (e.g., pressure of probe, location of measurement, etc.) to the post-processing analysis (e.g., removal of "bad" measurements, fitting to closed-form models, interpreting the measurement in the context of histology, etc.). Due to the large number of potential metadata types to be recorded and reported, it is quite cumbersome and time consuming for a research team to be able to do. Therefore, more work is needed to study the effect of these parameters, and to reach a consensus on what are the actual minimum types of metadata needed.

5 Conclusions and Future Steps

The measurement of the dielectric properties of biological tissues continues to be an important topic, with measurement data being broadly used across industry and academia in optimizing and improving existing technologies, developing new devices, and in assessing the safety of these technologies. However, there have been concerns over the consistency and validity of reports of dielectric data on tissues, promoting the desire for a standard measurement technique and standardized reporting framework. This work has aimed to progress the discussion of identifying standard approaches and, more importantly, identifying the hurdles and work to be done in order to achieve a consensus on standard approaches.

We have critically reviewed and examined the main measurement techniques that have been used to measure the dielectric properties of tissues in the literature to date. While there are several existing techniques available that can be used for measuring the dielectric properties of tissues, they all face limitations in terms of what types of samples can be measured or what types of measurements can be conducted. Emerging technologies for measuring the dielectric properties of tissues face similar constraints and are not yet well-validated.

However, beyond the lack of an "ideal" technique that can do-it-all, there are significant challenges in creating standards in this field. For example, consistency in measurement validation would enable the setting of standard "test cases" used to obtain the accuracy of a measurement system. However, there are currently no good options for test materials that encapsulate the variety of features found in actual tissues that can impact measurement accuracy. Furthermore, consistency in reporting metadata would support reusability of data and ease in comparing data. Notably, there are a significant number of parameters to consider, including all details regarding the tissue source, sample handling and processing, measurement protocol, and post-processing. However, at present, there is no consensus on the metadata parameters that are necessary to report, and those which can be neglected, without hindering the reusability or interpretability of a study.

Despite these gaps, and pending future work on strategies to address them, we can safely recommend increased adherence to high-quality procedures and reporting—including reporting of validation measurements and test scenarios to demonstrate the accuracy of a measurement method and reporting of as much metadata as possible—as the most important need in this field at this time.

Conflict of Interest

There are no conflicts of interest. This article does not include research in which human participants were involved. Informed consent not applicable. This article does not include any research in which animal participants were involved.

Data Availability Statement

The authors attest that all data for this study are included in the paper.

References

[1] IEEE, 2019, "C95.1-2019—IEEE Standard for Safety Levels with Respect to Human Exposure to Electric, Magnetic, and Electromagnetic Fields, 0 Hz to 300 GHz," IEEE, pp. 1–310.

[2] Mansouri, S., Alharbi, Y., Haddad, F., Chabcoub, S, Alshrouf, A., and Abd-Elghany, A. A., 2021, "Electrical Impedance Tomography—Recent Applications and Developments," J. Electr. Bioimpedance, **12**(1), pp. 50–62.

[3] Wu, Y., Hanzaee, F. F., Jiang, D., Bayford, R. H., and Demosthenous, A., 2021, "Electrical Impedance Tomography for Biomedical Applications: Circuits and Systems Review," IEEE Open J. Circuits Syst., **2**, pp. 380–397.

[4] Brown, B. H., 2003, "Electrical Impedance Tomography (EIT): A Review," J. Med. Eng. Technol., **27**(3), pp. 97–108.

[5] Bolomey, J.-C., 2018, "Crossed Viewpoints on Microwave-Based Imaging for Medical Diagnosis: From Genesis to Earliest Clinical Outcomes," *The World of Applied Electromagnetics*, A. Lakhtakia and C. M. Furse, eds., Springer International Publishing, Cham, Switzerland, pp. 369–414.

[6] O'Loughlin, D., O'Halloran, M., Moloney, B., Glavin, M., Jones, E., and Elahi, M. A., 2018, "Microwave Breast Imaging: Clinical Advances and Remaining Challenges," IEEE Trans. Biomed. Eng., **65**(11), pp. 2580–2590.

[7] Porter, E., Raterink, A., and Farshkaran, A., 2022, "Microwave-Based Detection of the Bladder State as a Support Tool for Urinary Incontinence," IEEE Antennas Propag. Mag., **64**(1), pp. 112–122.

[8] Guo, L., Alqadami, A. S. M., and Abbosh, A., 2023, "Stroke Diagnosis Using Microwave Techniques: Review of Systems and Algorithms," IEEE J. Electromagn. RF Microw. Med. Biol., **7**(2), pp. 122–135.

[9] Brace, C. L., 2010, "Microwave Tissue Ablation: Biophysics, Technology and Applications," Crit. Rev. Biomed. Eng., **38**(1), pp. 65–78.

[10] Rodrigues, D. B., Dobsicek-Trefna, H., Curto, S., Winter, L., Molitoris, J. K., Vrba, J., Vrba, D., Sumser, K., and Paulides, M. M., 2022, "Radiofrequency and Microwave Hyperthermia in Cancer Treatment," *Principles and Technologies for Electromagnetic Energy Based Therapies*, Academic Press, London, UK, pp. 281–311.

[11] Hasgall, P. A., Neufeld, E., Gosselin, M. C., Klingenböck, A., Kuster, N., Kuster, N., Hasgall, P., and Gosselin, M., 2022, "IT'IS Database for Thermal and Electromagnetic Parameters of Biological Tissues," Version 4.1, vol. itis.swiss/database.

[12] ITIS Foundation, 2023, "Database of Tissue Properties," https://itis.swiss/virtual-population/tissue-properties/database/dielectric-properties/

[13] Gabriel, C., Gabriel, S., and Corthout, E., 1996, "The Dielectric Properties of Biological Tissues: I. Literature Survey," Phys. Med. Biol., **41**(11), pp. 2231–2249.

[14] Gabriel, S., Lau, R. W., and Gabriel, C., 1996, "The Dielectric Properties of Biological Tissues: II. Measurements in the Frequency Range 10 Hz to 20 GHz," Phys. Med. Biol., **41**(11), pp. 2251–2269.

[15] Gabriel, S., Lau, R. W., and Gabriel, C., 1996, "The Dielectric Properties of Biological Tissues: III. Parametric Models for the Dielectric Spectrum of Tissues," Phys. Med. Biol., **41**(11), pp. 2271–2293.

[16] Sasaki, K., Porter, E., Rashed, E. A., Farrugia, L., and Schmid, G., 2022, "Emily Porter [HTML] From iop.org Measurement and Image-Based Estimation of Dielectric Properties of Biological Tissues—Past, Present, and Future—," Phys. Med. Biol., **67**(14), pp. 1–39.

[17] La Gioia, A., Porter, E., Merunka, I., Shahzad, A., Salahuddin, S., Jones, M., and O'Halloran, M., 2018, "Open-Ended Coaxial Probe Technique for Dielectric Measurement of Biological Tissues: Challenges and Common Practices," Diagnostics, **8**(2), pp. 1–38.

[18] Farrugia, L., Porter, E., Conceição, R. C., Meo, S. D., Godinho, D. M., Bonello, J., Ragulskis, M., et al., 2024, "The Complex Permittivity of Biological Tissues: A Practical Measurement Guideline," IEEE Access, **12**, pp. 10296–10314.
[19] Porter, E., La Gioia, A., Salahuddin, S., Decker, S., Shahzad, A., Elahi, M. A., O'Halloran, M., and Beyan, O., 2017, "Minimum Information for Dielectric Measurements of Biological Tissues (MINDER): A Framework for Repeatable and Reusable Data," Int. J. RF Microwave Comput. Aided Eng., **28**(3), p. e21201.
[20] Cilia, F., Di Meo, S., Farrugia, L., Bonello, J., Farhat, I., Dimech, E. J., Pasian, M., and Sammut, C. V., 2022, "Techniques for Temperature-Dependent Dielectric Measurements: A Review," Proceedings of the Microwave Mediterranean Symposium (MMS), Pizzo Calabro, Italy, May 9–13, pp. 1–4.
[21] Yaw, K. C., 2012, "Measurement of Dielectric Material Properties. Application Note," Rohde & Schwarz.
[22] Reinecke, T., Hagemeier, L., Schulte, V., Klintschar, M., and Zimmermann, S., 2013, "Quantification of Edema in Human Brain Tissue by Determination of Electromagnetic Parameters," Proceedings of the IEEE Sensors, Baltimore, MD, Nov. 3–6, pp. 1–4.
[23] Agilent Technologies, 2006, "Basics of Measuring the Dielectric Properties of Materials: Application Note," Agilent Technologies, Inc.
[24] Rohde & Schwarz, "Measurement of Dielectric Material Properties: Application Note," Rohde & Schwarz GmbH, https://cdn.rohde-schwarz.com/pws/dl_downloads/dl_application/00aps_undefined/RAC-0607-0019_1_5E.pdf, Accessed January 23, 2021.
[25] Roberts, S., and von Hippel, A., 1946, "A New Method for Measuring Dielectric Constant and Loss in the Range of Centimetre Waves," J. Appl. Phys., **17**(7), pp. 610–616.
[26] Foster, K. R., Schepps, J. L., Stoy, R. D., and Schwan, H. P., 1979, "Dielectric Properties of Brain Tissue Between 0.01 and 10 GHz," Phys. Med. Biol., **24**(6), pp. 1177–1187.
[27] Gregory, A. P., and Clarke, R. N., 2006, "A Review of RF and Microwave Techniques for Dielectric Measurements on Polar Liquids," IEEE Trans. Dielectr. Electr. Insul., **13**(4), pp. 727–743.
[28] Nicolson, A., and Ross, G. F., 1970, "Measurement of the Intrinsic Properties of Materials by Time-Domain Techniques," IEEE Trans. Instrum. Meas., **19**(4), pp. 377–382.
[29] Weir, W. B., 1974, "Automatic Measurement of Complex Dielectric Constant and Permeability," Proc. IEEE, **62**(1), pp. 33–36.
[30] Baker-Jarvis, J., Vanzura, E. J., and Kissick, W. A., 1990, "Improved Technique for Determining Complex Permittivity With the Transmission/Reflection Method," IEEE Trans. Microwave Theory Tech., **38**(8), pp. 1096–1103.
[31] Kim, S., and Baker-Jarvis, J., 2014, "An Approximate Approach To Determining the Permittivity and Permeability Near λ/2 Resonances in Transmission/Reflection Measurements," Prog. Electromagn. Res. B, **58**, pp. 95–109.
[32] Boughriet, A. H., Legrand, C., and Chapoton, A., 1997, "Noniterative Stable Transmission/Reflection Method for Low-Loss Material Complex Permittivity Determination," IEEE Trans. Microwave Theory Tech., **45**(1), pp. 52–57.
[33] Baker-Jarvis, J., Janezic, M. D., Grosvenor Hr, J. H., and Geyer, R. G., 1993, *Transmission/Reflection and Short-Circuit Line Methods for Measuring Permittivity and Permeability*, NIST United States Department of Commerce Technology Administration, National Institute of Standards and Technology, Gaithersburg, MD.
[34] Faktorova, D., 2009, "Microwave Characterization of Frequency and Temperature Dependences of Beef Bone Dielectric Properties Using Waveguide Measurement System," Measurement 2009, Proceedings of the 7th International Conference, Smolenice, Slovakia, May 20–23, pp. 402–405.
[35] Schepps, J. L., and Foster, K. R., 1980, "The UHF and Microwave Dielectric Properties of Normal and Tumour Tissues: Variation in Dielectric Properties With Tissue Water Content," Phys. Med. Biol., **25**(6), pp. 1149–1159.
[36] Lin, J., 1975, "Microwave Properties of Fresh Mammalian Brain Tissues at Body Temperature," IEEE Trans. Biomed. Eng., **BME-22**(1), pp. 74–76.
[37] Sebastian, J. L., Munoz, S., Miranda, J. M., and RIbas, B., 2004, "A Simple Experimental Set-Up for the Determination of the Complex Dielectric Permittivity of Biological Tissues at Microwave Frequencies," Proceedings of the 34th European Microwave Conference, Amsterdam, The Netherlands, Oct. 11–15, pp. 661–664.
[38] Effendi, M. R., Prastio, R. P., Munir, A., and Mengko, T .L. R., 2020, "Transmission Phase-Shift Method for Complex Permittivity Determination of Biological Sample Performed Using X-Band Rectangular Waveguide," Proceedings of the IEEE Region 10 Conference, Osaka, Japan, Nov. 16–19, pp. 919–922.
[39] Karolkar, B. D., Behari, J., and Prim, A., 1985, "Biological Tissues Characterization at Microwave Frequencies," IEEE Trans. Microwave Theory Tech., **33**(1), pp. 64–66.
[40] Poletaev, L. I., Yuv, M., and Mikhailov, V. A., 1992, "Testing of Dielectric Properties of Biological Tissues in Microwave Range for Solving Matching Problems," Med. Prog. Technol., **18**(1–2), pp. 91–94.
[41] Edrich, J., and Hardee, P. C., 1975, "Complex Permittivity and Penetration Depth of Certain Biological Tissue Between 40 and 90 GHz," Proceedings of the IEEE-MTT-S International Microwave Symposium, Palo Alto, CA, May 12–14, pp. 288–290.
[42] Shimonov, G., Koren, A., Sivek, G., and Socher, E., 2018, "Electromagnetic Property Characterization of Biological Tissues at D-Band," IEEE Trans. Terahertz Sci. Technol., **8**(2), pp. 155–160.
[43] Lu, Y., Yu, J., and Ren, Y., 1994, "Dielectric Properties of Human Red Blood Cells in Suspension at Radio Frequencies," Bioelectromagnetics, **15**(6), pp. 589–591.
[44] Alison, J. M., and Sheppard, R. J., 1993, "Dielectric Properties of Human Blood at Microwave Frequencies," Phys. Med. Biol., **38**(7), pp. 971–978.
[45] Handoko, E., Fahdiran, R., Budi, S., Saptari, S. A., Humairrah, A., Alaydrus, M., Mutmainnah, Z., and Puspitaningrum, R., 2019, "Complex Permittivity, Complex Permeability and Microwave Absorption Properties of Human Blood," Proceedings of the 4th Annual Applied Science and Engineering Conference, Bali, Indonesia, Apr. 24, pp. 1–4.
[46] Duhamel, F., Huynen, I., and Vorst, A. V., 1997, "Measurements of Complex Permittivity of Biological and Organic Liquids up to 100 GHz," Proceedings of the IEEE MTT-S International Microwave Symposium Digest, Denver, CO, June 8–13, pp. 107–110.
[47] Arkhypova, K. A., Krasov, P. S., and Fisun, A. I., 2013, "Modified Waveguide Sensor for Millimeter Dielectric Study of Human Erythrocytes in Medical Research," Proceedings of the 2013 International Kharkov Symposium on Physics and Engineering of Microwaves, Millimeter and Submillimeter Waves, Kharkov, Ukraine, June 23–28, pp. 568–570.
[48] Peng, Z., Hwang, J. Y., and Andriese, M., 2014, "Maximum Sample Volume for Permittivity Measurements by Cavity Perturbation Technique," IEEE Trans. Instrum. Meas., **63**(2), pp. 450–445.
[49] Land, D. V., and Campbell, A. M., 1992, "A Quick Accurate Method for Measuring the Microwave Dielectric Properties of Small Tissue Samples," Phys. Med. Biol., **37**(1), pp. 183–192.
[50] Campbell, A., 1990, "Measurements and Analysis of the Microwave Dielectric Properties of Tissues," J. Appl. Phys., **22**, pp. 95.
[51] Keysight Technologies, 2020, "Application Note: Basics of Measuring the Dielectric Properties of Materials," Keysight Technologies, USA.
[52] Campbell, A., and Land, D. V., 1992, "Dielectric Properties of Female Human Breast Tissue Measured In Vitro at 3.2 GHz," Phys. Med. Biol., **37**(1), pp. 193–210.
[53] Che, W., Wang, Z., Chang, Y., and Russer, P., 2008, "Permittivity Measurement of Biological Materials With Improved Microwave Cavity Perturbation Technique," Proceedings of the 38th European Microwave Conference, Amsterdam, The Netherlands, Oct. 27–31, pp. 905–908.
[54] Ma, J. L., Wu, Z., Xia, Q., Wang, S., Tang, J., Wang, K., Guo, L., Jiang, H., Zeng, B., and Gong, Y., 2020, "Complex Permittivity Measurement of High-Loss Biological Material With Improved Cavity Perturbation Method in the Range of 26.5-40 GHz," Electronics, **9**(8), pp. 1–13.
[55] Rajasekharan, C., Girishkumar, C., Anil, L., Mathew, A. J., and Mathew, K. T., 2010, "Diagnostic Value of Microwaves in Neurological Disorders," J. Microwave Power Electromagn. Energy, **44**(3), pp. 139–143.
[56] Lonappan, A., Hamsakkutty, V., Bindu, G., Jacob, J., Thomas, V., and Mathew, K. T., 2004, "Dielectric Properties of Human Urine at Microwave Frequencies," Microwave Opt. Technol. Lett., **42**(6), pp. 500–503.
[57] Lonappan, A., Rajasekaran, C., Thomas, V., Bindu, G., and Mathew, K. T., 2007, "Determination of Pregnancy Using Microwaves," Microwave Opt. Technol. Lett., **49**(4), pp. 786–788.
[58] Lonappan, A., Bindu, G., Thomas, V., and Jacob, J., 2007, "Diagnosis of Diabetes Mellitus Using Microwaves," J. Electromagn. Waves Appl., **21**(10), pp. 1393–1401.
[59] Raveendranath, U., Kumar, S. B., Mathew, S., and Mathew, K. T., 1998, "Microwave Diagnosis of Diabetes in Human Beings Using Cavity Perturbation Technique," Proceedings of the International Conference on Microwave and Millimeter Wave Technology, Beijing, China, Aug. 18–20, pp. 803–806.
[60] Lonappan, A., 2012, "Novel Method of Detecting Pregnancy Using Microwaves," J. Electromagn. Anal. Appl., **4**(8), pp. 340–343.
[61] Jin, L., and Zhao, Q., 2010, "Microwave and Millimeter Wave Nondestructive Measurement in Biomedical Engineering," Proceedings of the 3rd International Conference on Biomedical Engineering and Informatics, Yantai, China, Oct. 16–18, pp. 1523–1527.
[62] Bindu, G., Abraham, S. J., Aanandan, C. K., and Mathew, K. T., 2006, "Microwave Characterization of Female Human Breast Tissues," Proceedings of the European Conference on Wireless Technology, Manchester, UK, Sept. 10–12, pp. 122–126.
[63] Wang, Z., Che, W. Q., and Chang, Y. M., 2008, "Permittivity Measurement of Biological Materials With Improved Microwave Cavity Perturbation Technique," Microwave Opt. Technol. Lett., **50**(7), pp. 1800–1804.
[64] Kumar, S. B., Mathew, K. T., Raveendranath, U., and Augustine, P., 2001, "Dielectric Properties of Certain Biological Materials at Microwave Frequencies," J. Microwave Power Electromagn. Energy, **36**(2), pp. 67–75.
[65] Misik, S., and Masszi, G., 1983, "Microwave Method for Determining Dielectric Parameters of Living Biological Objects. III. Study of Water Binding in Frog Nerve," Acta Biochim. Biophys., **18**(3–4), pp. 223–230.
[66] Robinson, M. P., and Pegg, D. E., 1999, "Rapid Electromagnetic Warming of Cells and Tissues," IEEE Trans. Biomed. Eng., **46**(12), pp. 1413–1425.
[67] Mosig, J. R., Besson, J. C., Gex-Fabry, M., and Gardiol, F. E., 1981, "Reflection of an Open-Ended Coaxial Line and Application to Non-Destructive Measurements of Materials," IEEE Trans. Instrum. Meas., **IM-30**(1), pp. 46–51.
[68] Levine, H., and Papas, C. H., 1951, "Theory of the Circular Diffraction Antenna," J. Appl. Phys., **22**(1), pp. 29–43.
[69] Misra, D. K., 1987, "A Quasi-Static Analysis of Open-Ended Coaxial Lines," IEEE Trans. Microwave Theory Tech., **MTT-35**(10), pp. 925–928.
[70] Stuchly, M. S., and Stuchly, S. S., 1980, "Coaxial Line Reflection Methods for Measuring Dielectric Properties of Biological Substances at Radio and

Microwave Frequencies—A Review," IEEE Trans. Instrum. Meas., **29**(3), pp. 176–183.
[71] Marsland, T. P., and Evans, S., 1987, "Dielectric Measurements With an Open-Ended Coaxial Probe," IEEE Proc., **134**(4), pp. 341–349.
[72] Bao, J. Z., Swicord, M. L., and Davis, C. C., 1996, "Microwave Dielectric Characterization of Binary Mixtures of Water, Methanol, and Ethanol," J. Chem. Phys., **104**(12), pp. 4441–4450.
[73] Wei, Y.-Z., and Sridhar, S., 1991, "Radiation-Corrected Open-Ended Coax Line Technique for Dielectric Measurements of Liquids up to 20 GHz," IEEE Trans. Microwave Theory Tech., **39**(3), pp. 526–531.
[74] Kraszewski, A., Stuchly, M., and Stuchly, S., 1983, "ANA Calibration Method for Measurements of Dielectric Properties," IEEE Trans. Instrum. Meas., **32**(2), pp. 385–387.
[75] Piuzzi, E., Merla, C., Cannazza, G., Zambotti, A., Apollonio, F., Cataldo, A., D'Atanasio, A., De Benedetto, E., and Liberti, M., 2013, "A Comparative Analysis Between Customized and Commercial Systems for Complex Permittivity Measurements on Liquid Samples at Microwave Frequencies," IEEE Trans. Instrum. Meas., **62**(5), pp. 1034–1046.
[76] Ruvio, G., Vaselli, M., Lopresto, L., Pinto, R., Farina, L., and Cavagnaro, M., 2018, "Comparison of Different Methods for Dielectric Properties Measurements in Liquid Sample Media," Int. J. RF Microwave Comput. Aided Eng., **28**(3), pp. 1–10.
[77] Cavagnaro, M., and Ruvio, G., 2020, "Numerical Sensitivity Analysis for Dielectric Characterization of Biological Samples by Open-Ended Probe Technique," Sensors, **20**(13), pp. 3756.
[78] La Gioia, A., Santorelli, A., Elahi, A., O'Halloran, M., and Porter, E., 2020, "Predicting the Sensing Radius of a Coaxial Probe Based on the Probe Dimensions," IEEE Trans. Antennas Propag., **68**(9), pp. 6704–6716.
[79] Porter, E., and O'Halloran, M., 2017, "Investigation of Histology Region in Dielectric Measurements of Heterogeneous Tissues," IEEE Trans. Antennas Propag., **65**(10), pp. 5541–5552.
[80] La Gioia, A., O'Halloran, M., and Porter, E., 2018, "Modelling the Sensing Radius of a Coaxial Probe for Dielectric Characterisation of Biological Tissues," IEEE Access, **6**, pp. 46516–46526.
[81] Aydinalp, C., Joof, S., and Yilmaz, T., 2021, "Towards Accurate Microwave Characterization of Tissues: Sensing Depth Analysis of Open-Ended Coaxial Probes With Ex Vivo Rat Breast and Skin Tissues," Diagnostics, **11**(2), pp. 1–19.
[82] Hagl, D. M., Popovic, D., Hagness, S. C., Booske, J. H., and Okoniewski, M., 2003, "Sensing Volume of Open-Ended Coaxial Probes for Dielectric Characterization of Breast Tissue at Microwave Frequencies," IEEE Trans. Microwave Theory Tech., **51**(4), pp. 1194–1206.
[83] Meaney, P. M., Gregory, A. P., Seppälä, J., and Lahtinen, T., 2016, "Open-Ended Coaxial Dielectric Probe Effective Penetration Depth Determination," IEEE Trans. Microwave Theory Tech., **64**(3), pp. 915–923.
[84] Maenhout, G., Markovic, T., Ocket, I., and Nauwelaers, B., 2020, "Settings Open AccessArticle Effect of Open-Ended Coaxial Probe-to-Tissue Contact Pressure on Dielectric Measurements," Sensors, **20**(7), pp. 1–13.
[85] Sasaki, K., Nishikata, A., Watanabe, S., and Fujiwara, O., 2018, "Intercomparison of Methods for Measurement of Dielectric Properties of Biological Tissues With a Coaxial Sensor at Millimiter-Wave Frequencies," Phys. Med. Biol., **63**(20), pp. 2–10.
[86] Speah, 2023, "DAK Overview," Speag, https://speag.swiss/products/dak/overview/.
[87] Xu, D., Liu, L., and Jiang, Z., 1987, "Measurement of the Dielectric Properties of Biological Substances Using an Improved Open-Ended Coaxial Line Resonator Method," IEEE Trans. Microwave Theory Tech., **MTT-35**(12), pp. 1424–1428.
[88] Zajicek, R., and Vrba, J., 2010, "Broadband Complex Permittivity Determination for Biomedical Applications, in Advanced Microwave Circuits and Systems," *Advanced Microwave Circuits and Systems, Chap. 17*, V. Zhurbenko, ed., Intech-Open, Croatia, pp. 365–385.
[89] Salahuddin, S., Porter, E., Meaney, P. M., and O'Halloran, M., 2017, "Effect of Logarithmic and Linear Frequency Scales on Parametric Modelling of Tissue Dielectric Data," Biomed. Phys. Eng. Express, **3**(1), pp. 1–22.
[90] Liporace, F., and Cavagnaro, M., 2022, "Use of the Open-Ended Probe Technique for the Dielectric Characterization of Biological Tissues at Low Frequencies," Proceedings of 15th International Workshop on Impedance Spectroscopy (IWIS), Chemnitz, Germany, Sept. 27–30, pp. 66–69.
[91] Topsakal, E., Karacolak, T., and Moreland, E. C., 2011, "Glucose-Dependent Dielectric Properties of Blood Plasma," Proceedings of the XXXth URSI General Assembly and Scientific Symposium, Istanbul, Turkey, Aug. 13–20, pp. 1–4.
[92] Salahuddin, S., O'Halloran, M., Farrugia, L., Bonello, J., Wismayer, P. S., Sammut, C. V., and Porter, E., 2017, "Effects of Standard Coagulant Agents on the Dielectric Properties of Fresh Human Blood," IEEE Trans. Dielectr. Electr. Insul., **24**(5), pp. 3283–3289.
[93] Dunne, E., O'Halloran, M., Porter, E., Bonello, J., Farrugia, L., Sammut, C. V., and Schembri-Wismayer, P., 2019, "Heparin as an Anticoagulant for the Dielectric Measurement of Blood," IEEE Trans. Dielectr. Electr. Insul., **26**(1), pp. 228–234.
[94] Santorelli, A., Fitzgerald, S., Douglas, A., Doyle, K., and O'Halloran, M., 2020, "Dielectric Profile of Blood Clots to Inform Ischemic Stroke Treatments," Proceedings of the 42nd Annual International Conference of the IEEE Engineering in Medicine & Biology Society (EMBC), Montreal, Canada, July 20–24, pp. 3723–3726.
[95] Mun, P. S., Ting, H. N., Ong, T. A., Wong, C. M., Ng, K. H., and Chong, Y. B., 2015, "A Study of Dielectric Properties of Proteinuria Between 0.2 GHz and 50 GHz," PLoS One, **10**(6), pp. 1–12.
[96] Zhu, C.-Z., Ting, H.-N., and Ng, K. H., 2018, "Detection of Pregnancy Using Dielectric Properties of Urine," J. Microwave Power Electromagn. Energy, **52**(3), pp. 182–197.
[97] Martellosio, A., Bellomi, M., Pasian, M., Bozzi, M., Perregrini, L., Mazzanti, A., Svelto, F., Summers, P. E., Renne, G., and Preda, L., 2017, "Dielectric Properties Characterization From 0.5 to 50 GHz of Breast Cancer Tissues," IEEE Trans. Microwave Theory Tech., **65**(3), pp. 998–1011.
[98] Lazebnik, M., Popovic, D., McCartney, L., Watkins, C. B, Lindstrom, M. J, Harter, J., Sewall, S., et al., 2007, "A Large-Scale Study of the Ultrawideband Microwave Dielectric Properties of Normal, Benign and Malignant Breast Tissues Obtained From Cancer Surgeries," Phys. Med. Biol., **52**(20), pp. 6093–6115.
[99] Lazebnik, M., McCartney, L., Popovic, D., Watkins, C. B, Lindstrom, M. J, Harter, J., Sewall, S., et al., 2007, "A Large-Scale Study of the Ultrawide Band Microwave Dielectric Properties of Normal Breast Tissue Obtained From Reduction Surgeries," Phys. Med. Biol., **52**(10), pp. 2637–2656.
[100] Peyman, A., Kos, B., Djokić, M., Trotovšek, B., Limbaeck-Stokin, C., Serša, G., and Miklavčič, D., 2015, "Variation in Dielectric Properties Due to Pathological Changes in Human Liver," Bioelectromagnetics, **36**(8), pp. 603–612.
[101] Amin, B., Shahzad, A., Farina, L., Parle, E., McNamara, L., O'Halloran, M., and Elahi, M. A., 2020, "Dielectric Characterization of Diseased Human Trabecular Bones at Microwave Frequency," Med. Eng. Phys., **78**, pp. 21–28.
[102] Irastorza, R. M., Blangino, E., Carelvaro, C. M., and Vericat, F., 2014, "Modeling of the Dielectric Properties of Trabecular Bone Samples at Microwave Frequency," Med. Biol. Eng. Comput., **52**(5), pp. 439–477.
[103] Peyman, A., Gabriel, C., Grant, E. H., Vermeeren, G., and Martens, L., 2009, "Institute of Physics and Engineering in Medicine, Find Out More Variation of the Dielectric Properties of Tissues With Age: The Effect on the Values of SAR in Children When Exposed to Walkie–Talkie Devices," Phys. Med. Biol., **54**(2), pp. 227–241.
[104] Halter, R. J., Zhou, T., Meaney, P. M., Hartov, A., Barth, R. J., Rosenkranz, K. M., Wells, W. A., et al., 2009, "The Correlation of In Vivo and Ex Vivo Tissue Dielectric Properties to Validate Electromagnetic Breast Imaging: Initial Clinical Experience," Physiol. Meas., **30**(6), pp. S121–S136.
[105] Mohammed, B. J., Manoufali, M., Naqvi, S. A. R., Bialkowski, K. S., Mills, P. C., and Abbosh, A. M., 2020, "Using Dielectric Properties of Solid Fraction and Water Content to Characterize Tissues at Different Health and Age Conditions," IEEE J. Electromagn. RF Microw. Med. Biol., **4**(1), pp. 69–77.
[106] Farrugia, L., Wismayer, P. S., Mangion, L. Z., and Sammut, C. V., 2016, "Accurate In Vivo Dielectric Properties of Liver From 500 MHz to 40 GHz and Their Correlation to Ex Vivo Measurements," Electromagn. Biol. Med., **35**(4), pp. 365–373.
[107] Halter, R. J., Hartov, A., Heaney, J. A., Paulsen, K. D., and Schned, A. R., 2007, "Electrical Impedance Spectroscopy of the Human Prostate," IEEE Trans. Biomed. Eng., **54**(7), pp. 1321–1327.
[108] Park, J., Choi, W. M., Kim, K., Jeong, W. I., Seo, J. B., and Park, I., 2018, "Biopsy Needle Integrated With Electrical Impedance Sensing Microelectrode Array Towards Real-Time Needle Guidance and Tissue Discrimination," Sci. Rep., **8**, pp. 1–12.
[109] Rigaud, B., Hamzaoui, L., Chauveau, N., Granie, M., Di Rinaldi, J. P. S., and Morucci, J. P., 1994, "Tissue Characterization by Impedance: A Multifrequency Approach," Physiol. Meas., **15**(2A), pp. A13–A20.
[110] Haemmerich, D., Staelin, S. T., Tsai, J. Z., Tungjitkusolmun, S., and Mahvi, D. M., 2003, "In Vivo Electrical Conductivity of Hepatic Tumours," Physiol. Meas., **24**(2), pp. 251–260.
[111] Park, J., Sempionatto, J. R., Kim, J., Jeong, Y., Gu, J., Wang, J., and Park, I., 2020, "Microscale Biosensor Array Based on Flexible Polymeric Platform Toward Lab-on-a-Needle: Real-Time Multiparameter Biomedical Assays on Curved Needle Surfaces," ACS Sens., **5**(5), pp. 1363–1373.
[112] Tsai, J. Z., Cao, H., Tungjitkusolmun, S., Woo, E. J., Vorperian, V. R., and Webster, J. G., 2000, "Dependence of Apparent Resistance of Four-Electrode Probes on Insertion Depth," IEEE Trans. Biomed. Eng., **47**(1), pp. 41–48.
[113] Halter, R., Hartov, A., and Paulsen, K. D., 2004, "Design and Implementation of a High Frequency Electrical Impedance Tomography System," Physiol. Meas., **25**(1), pp. 379–390.
[114] Laufer, S., Ivorra, A., Reuter, V. E., Rubinsky, B., and Solomon, S. B., 2010, "Electrical Impedance Characterization of Normal and Cancerous Human Hepatic Tissue," Physiol. Meas., **31**(7), pp. 995–1009.
[115] Haemmerich, D., Schutt, D. J., Wright, A. W., Webster, J. G., and Mahvi, D. M., 2009, "Electrical Conductivity Measurement of Excised Human Metastatic Liver Tumours Before and After Thermal Ablation," Physiol. Meas., **30**(5), pp. 459–466.
[116] Tsai, J. Z., Will, J. A., Hubbard-Van Stelle, S., Cao, H., Tungjitkusolmun, S., Choy, Y. B., Haemmerich, D., Vorperian, V. R., and Webster, J. G., 2002, "In-Vivo Measurement of Swine Myocardial Resistivity," IEEE Trans. Biomed. Eng., **49**(5), pp. 472–483.
[117] Gabriel, C., Peyman, A., and Grant, E. H., 2009, "Electrical Conductivity of Tissue at Frequencies Below 1 MHz," Phys. Med. Biol., **54**(16), pp. 4863–4878.
[118] Teixeira, V. S., Labitzky, V., Schumacher, U., and Krautschneider, W., 2020, "Use of Electrical Impedance Spectroscopy to Distinguish Cancer From Normal Tissues with a Four Electrode Terminal Setup," Curr. Dir. Biomed. Eng., **6**(3), pp. 341–344.

[119] Zurbuchen, U., Holmer, C., Lehmann, K. S., Stein, T., Roggan, A., Seifarth, C., Buhr, H.-J., and Ritz, J.-P., 2010, "Determination of the Temperature-Dependent Electric Conductivity of Liver Tissue Ex Vivo and In Vivo: Importance for Therapy Planning for the Radiofrequency Ablation of Liver Tumours," Int. J. Hyperthermia, **26**(1), pp. 26–33.
[120] Meaney, P. M., Rydholm, T., and Brisby, H., 2018, "A Transmission-Based Dielectric Property Probe for Clinical Applications," Sensors, **18**(10), pp. 1–16.
[121] Meaney, P. M., Gregory, A., Epstein, N., and Paulsen, K. D., 2014, "Microwave Open-Ended Coaxial Dielectric Probe: Interpretation of the Sensing Volume Re-Visited," BMC Med. Phys., **14**(3), pp. 1–11.
[122] Peyman, A., and Gabriel, C., 2010, "Cole-Cole Parameters for the Dielectric Properties of Porcine Tissues as a Function of Age at Microwave Frequencies," Phys. Med. Biol., **55**(15), pp. N412–N419.
[123] Savazzi, M., Porter, E., O'Halloran, M., Costa, J. R., Fernandes, C. A., Felicio, J. M., and Conceicao, R. C., 2020, "Development of a Transmission-Based Open-Ended Coaxial-Probe Suitable for Axillary Lymph Node Dielectric Measurements," Proceedings of the 2020 14th European Conference on Antennas and Propagation (EuCAP), Copenhagen, Denmark, Mar. 15–20, pp. 1–5.
[124] Bayford, R. H., 2006, "Bioimpedance Tomography (Electrical Impedance Tomography)," Annu. Rev. Biomed. Eng., **8**(1), pp. 63–91.
[125] Lee, M. H., Jang, G. Y., Kim, Y. E., Yoo, P. J., Wi, H., Oh, T. I., and Woo, E. J., 2018, "Portable Multi-Parameter Electrical Impedance Tomography for Sleep Apnea and Hypoventilation Monitoring: Feasibility Study," Physiol. Meas., **39**(12), pp. 124004.
[126] Wan, Y., Borsic, A., Heaney, J., Seigne, J., Schned, A., Baker, M., Wason, S., Hartov, A., and Halter, R., 2013, "Transrectal Electrical Impedance Tomography of the Prostate: Spatially Coregistered Pathological Findings for Prostate Cancer Detection," Med. Phys., **40**(6Part1), pp. 063102.
[127] Meroni, D., Maglioli, C. C., Bovio, D., Greco, F. G., and Aliverti, A., 2017, "An Electrical Impedance Tomography (EIT) Multi-Electrode Needle-Probe Device for Local Assessment of Heterogeneous Tissue Impeditivity," Proceedings of the Annual International Conference of the IEEE Engineering in Medicine and Biology Society, Jeju, South Korea, July 11–15, pp. 1385–1388.
[128] McDermott, B., Elahi, A., Santorelli, A., O'Halloran, M., Avery, J., and Porter, E., 2020, "Multi-Frequency Symmetry Difference Electrical Impedance Tomography With Machine Learning for Human Stroke Diagnosis," Physiol. Meas., **41**(7), p. 075010.
[129] Yang, L., Liu, W., Chen, R., Zhang, G., Li, W., Fu, F., and Dong, X., 2017, "In Vivo Bioimpedance Spectroscopy Characterization of Healthy, Hemorrhagic and Ischemic Rabbit Brain Within 10 Hz-1 MHz," Sensors, **17**(4), pp. E791.
[130] Schlebusch, T., Nienke, S., Leonhardt, S., and Walter, M., 2014, "Bladder Volume Estimation From Electrical Impedance Tomography," Physiol. Meas., **35**(9), pp. 1813–1823.
[131] Dunne, E., Santorelli, A., McGinley, B., Leader, G., O'Halloran, M., and Porter, E., 2018, "Image-Based Classification of Bladder State Using Electrical Impedance Tomography," Physiol. Meas., **39**(12), pp. 124001.
[132] Nguyen, D. T., Jin, C., Thiagalingam, A., and McEwan, A. L., 2012, "A Review on Electrical Impedance Tomography for Pulmonary Perfusion Imaging," Physiol Meas., **33**(5), pp. 695–706.
[133] Frerichs, I., Amato, M. B. P., van Kaam, A. H., Tingay, D. G., Zhao, Z., Grychtol, B., Bodenstein, M., et al., 2017, "Chest Electrical Impedance Tomography Examination, Data Analysis, Terminology, Clinical Use and Recommendations: Consensus Statement of the TRanslational EIT DevelopmeNt StuDy Group," Thorax, **72**(1), pp. 83–93.
[134] Murphy, E. K., Mahara, A., Khan, S., Hyams, E. S., Schned, A. R., Pettus, J., and Halter, R. J., 2017, "Comparative Study of Separation Between ex Vivo Prostatic Malignant and Benign Tissue Using Electrical Impedance Spectroscopy and Electrical Impedance Tomography," Physiol. Meas., **38**(6), pp. 1242–1261.
[135] Halter, R. J., Hartov, A., Poplack, S. P., diFlorio-Alexander, R., Wells, W. A., Rosenkranz, K. M., Barth, R. J., Kaufman, P. A., and Paulsen, K. D., 2015, "Real-Time Electrical Impedance Variations in Women With and Without Breast Cancer," IEEE Trans. Med. Imaging, **34**(1), pp. 38–48.
[136] Brazey, B., Haddab, Y., Koebel, L., and Zemiti, N., 2022, "Electrical Impedance Tomography: A Potential Tool for Intraoperative Imaging of the Tongue Base," Physiol. Meas., **43**(1), p. 015008.
[137] Liu, J., Wang, Y., Katscher, U., and He, B., 2017, "Electrical Properties Tomography Based on Maps in MRI: Principles, Applications, and Challenges," IEEE Trans. Biomed. Eng., **64**(11), pp. 2515–2530.
[138] Katscher, U., Kim, D. H., and Seo, J. K., 2013, "Recent Progress and Future Challenges in MR Electric Properties Tomography," Comput. Math. Methods Med., **2013**, p. 546562.
[139] Katscher, U., and van den Berg, C. A. T., 2017, "Electric Properties Tomography: Biochemical, Physical and Technical Background, Evaluation and Clinical Applications," NMR Biomed., **30**(8), pp. 1–15.
[140] Ropella, K. M., and Noll, D. C., 2017, "A Regularized, Model-Based Approach to Phase-Based Conductivity Mapping Using MRI," Magn. Reson. Med., **78**(5), pp. 2011–2021.
[141] Leijsen, R. L., Brink, W. M., van den Berg, C. A. T., Webb, A. G., and Remis, R. F., 2018, "3-D Contrast Source Inversion-Electrical Properties Tomography," IEEE Trans. Med. Imaging, **37**(9), pp. 2080–2089.
[142] van Lier, A., Raaijmakers, A., Voigt, T., Lagendijk, J. J. W., Luijten, P. R., Katscher, U., and van den Berg, C. A. T., 2014, "Electrical Properties Tomography in the Human Brain at 1.5, 3, and 7T: A Comparison Study," Magn. Reson. Med., **71**(1), pp. 354–363.
[143] Serralles, J. C., Lattanzi, R., Giannakopoulos, I. I., Zhang, B., Ianniello, C., Cloos, M. A., Polimeridis, A. G., White, J. K., Sodickson, D. K., and Daniel, L., 2020, "Noninvasive Estimation of Electrical Properties From Magnetic Resonance Measurements via Global Maxwell Tomography and Match Regularization," IEEE Trans. Biomed. Eng., **67**(1), pp. 3–15.
[144] Duan, S., Zhu, Y., Liu, F., and Xin, S. X., 2020, "Numerical Experiments on the Contrast Capability of Magnetic Resonance Electrical Property Tomography," Magn. Reson. Med. Sci., **19**(1), pp. 77–85.
[145] Wang, Y., Shao, Q., Van de Moortele, P.-F., Racila, E., Liu, J., Bischof, J., and He, B., 2019, "Mapping Electrical Properties Heterogeneity of Tumor Using Boundary Informed Electrical Properties Tomography (BIEPT) at 7 T," Magn. Reson. Med., **81**(1), pp. 393–409.
[146] Michel, E., Hernandez, D., and Lee, S. Y., 2017, "Electrical Conductivity and Permittivity Maps of Brain Tissues Derived From Water Content Based on T 1 -Weighted Acquisition," Magn. Reson. Med., **77**(3), pp. 1094–1103.
[147] Mandija, S., Sbrizzi, A., Katscher, U., Luijten, P. R., and van den Berg, C. A. T., 2018, "Error Analysis of Helmholtz-Based MR-Electrical Properties Tomography," Magn. Reson. Med., **80**(1), pp. 90–100.
[148] Gavazzi, S., Shcherbakova, Y., Bartels, L. W., Stalpers, L. J. A., Lagendijk, J. J. W., Crezee, H., van den Berg, C. A. T., and van Lier, A. L. H. M. W., 2020, "Transceive Phase Mapping Using the PLANET Method and Its Application for Conductivity Mapping in the Brain," Magn. Reson. Med., **83**(2), pp. 590–607.
[149] Stijnman, P. R. S., Mandija, S., Fuchs, P. S., van den Berg, C. A. T., and Remis, R. F., 2021, "Transceive Phase Corrected 2D Contrast Source Inversion-Electrical Properties Tomography," Magn. Reson. Med., **85**(5), pp. 2856–2868.
[150] Fuchs, P. S., Mandija, S., Stijnman, P. R. S., Brink, W. M., van den Berg, C. A. T., and Remis, R. F., 2018, "First-Order Induced Current Density Imaging and Electrical Properties Tomography in MRI," IEEE Trans. Comput. Imaging, **4**(4), pp. 624–631.
[151] Liu, J., Zhang, X., Schmitter, S., Van de Moortele, P.-F., and He, B., 2015, "Gradient-Based Electrical Properties Tomography (gEPT): A Robust Method for Mapping Electrical Properties of Biological Tissues In Vivo Using Magnetic Resonance Imaging," Magn. Reson. Med., **74**(3), pp. 634–646.
[152] Arduino, A., Bottauscio, O., Chiampi, M., and Zilberti, L., 2019, "Uncertainty Propagation in Phaseless Electric Properties Tomography," Proceedings of the International Conference on Electromagnetics in Advanced Applications, Granada, Spain, Sept. 9–13, pp. 412–415.
[153] Arduino, A., 2021, "EPTlib: An Open-Source Extensible Collection of Electric Properties Tomography Techniques," Appl. Sci., **11**(7), pp. 1–21.
[154] Kim, D.-H., Choi, N., Gho, S.-M., Shin, J., and Liu, C., 2013, "Simultaneous Imaging of In Vivo Conductivity and Susceptibility," Magn. Reson. Med., **71**(3), pp. 1144–1150.
[155] Kim, D.-H., Chauhan, M., Kim, M.-O., Jeong, W. C., Kim, H. J., Sersa, I., Kwon, O. I., and Woo, E. J., 2015, "Frequency-Dependent Conductivity Contrast for Tissue Characterization Using a Dual-Frequency Range Conductivity Mapping Magnetic Resonance Method," IEEE Trans. Med. Imaging, **34**(2), pp. 507–513.
[156] Shin, J., Kim, M.-O., Cho, S., and Kim, D.-H., 2017, "Fast Spin Echo Imaging-Based Electric Property Tomography With K-Space Weighting via T2 Relaxation (rEPT)," IEEE Trans. Med. Imaging, **36**(8), pp. 1615–1625.
[157] Shin, J., Kim, J.-H., and Kim, D.-H., 2018, "Redesign of the Laplacian Kernel for Improvements in Conductivity Imaging Using MRI," Magn. Reson. Med., **81**(3), pp. 2167–2175.
[158] Mandija, S., Meliado, E. F., Huttinga, N. R. F., Luijten, P. R., and van den Berg, C. A. T., 2019, "Opening a New Window on MR-Based Electrical Properties Tomography with Deep Learning," Sci. Rep., **9**(8895), pp. 1–9.
[159] Gavazzi, S., van den Berg, C. A. T., Savenije, M. H. F., Kok, H. P., de Boer, P., Stalpers, L. J. A., Lagendijk, J. J. W., Crezee, H., and van Lier, A. L. H. M. W., 2020, "Deep Learning-Based Reconstruction of In Vivo Pelvis Conductivity With a 3D Patch-Based Convolutional Neural Network Trained on Simulated MR Data," Magn. Reson. Med., **84**(5), pp. 2772–2787.
[160] Hampe, N., Katscher, U., van den Berg, C. A T, Tha, K. K., and Mandija, S., 2020, "Investigating the Challenges and Generalizability of Deep Learning Brain Conductivity Mapping," Phys. Med. Biol., **65**(13), pp. 1–20.
[161] Jung, K.-J., Mandija, S., Kim, J. H., Ryu, K., Jung, S., Cui, C., Kim, S. Y., Park, M., van den Berg, C. A., and Kim, D. H., 2021, "Improving Phase-Based Conductivity Reconstruction by Means of Deep Learning–Based Denoising of B1 + Phase Data for 3 T MRI," Magn. Reson. Med., **86**(4), pp. 2084–2094.
[162] Leijsen, R., van den Berg, C., Webb, A., Remis, R., and Mandija, S., 2019, "Combining Deep Learning and 3D Contrast Source Inversion in MR-Based Electrical Properties Tomography," NMR Biomed., **35**(4), pp. 1–7.
[163] Tha, K. K., Katscher, U., Yamaguchi, S., Stehning, C., Terasaka, S., Fujima, N., Kudo, K., et al., 2018, "Noninvasive Electrical Conductivity Measurement by MRI: A Test of Its Validity and the Electrical Conductivity Characteristics of Glioma," Eur. Radiol., **28**(1), pp. 348–355.
[164] Mandija, S., Petrov, P. I., Vink, J. J. T., Neggers, S. F. W., and van den Berg, C. A. T., 2021, "Brain Tissue Conductivity Measurements With MR-Electrical Properties Tomography: An In Vivo Study," Brain Topogr., **34**(1), pp. 56–63.
[165] Lesbats, C., Katoch, N., Minhas, A. S., Taylor, A., Kim, H. J., Woo, E. J., and Poptani, H., 2021, "High-frequency Electrical Properties Tomography at 9.4 T as a Novel Contrast Mechanism for Brain Tumors," Magn. Reson. Med., **86**(1), pp. 382–392.
[166] Kim, S.-Y., Shin, J, Kim, D.-H., Kim, M. J., Kim, E.-K., Moon, H. J., and Yoon, J. H., 2016, "Correlation Between Conductivity and Prognostic Factors in

Invasive Breast Cancer Using Magnetic Resonance Electric Properties Tomography (MREPT)," Eur. Radiol., **26**(7), pp. 2317–2326.
[167] Shin, J., Kim, M. J., Lee, J., Nam, Y., Kim, M.-O., Choi, N., Kim, S., and Kim, D.-H., 2015, "Initial Study on In Vivo Conductivity Mapping of Breast Cancer Using MRI," J. Magn. Reson. Imaging, **42**(2), pp. 371–378.
[168] Mori, N., Tsuchiya, K., Sheth, D., Mugikura, Sh., Takase, K., Katscher, U., and Abe, H.,, 2019, "Diagnostic Value of Electric Properties Tomography (EPT) for Differentiating Benign From Malignant Breast Lesions: Comparison With Standard Dynamic Contrast-Enhanced MRI," Eur. Radiol., **29**(4), pp. 1778–1786.
[169] Kim, S.-Y., Shin, J., Kim, D.-H., Kim, E.-K., Moon, H. J., Yoon, J. H., You, J. K., and Kim, M. J., 2018, "Correlation Between Electrical Conductivity and Apparent Diffusion Coefficient in Breast Cancer: Effect of Necrosis on Magnetic Resonance Imaging," Eur. Radiol., **28**(8), pp. 3204–3214.
[170] Balidemaj, E., de Boer, P., van Lier, A. L. H. M. W., Remis, R. F., Stalpers, L. J. A., Westerveld, G. H., Nederveen, A. J., van den Berg, C. A. T., and Crezee, J., 2016, "In Vivo Electric Conductivity of Cervical Cancer Patients Based on B_1^+ Maps at 3 T MRI," Phys. Med. Biol., **61**(4), pp. 1596–1607.
[171] Balidemaj, E., Kok, H. P., Schooneveldt, G., van Lier, A. L. H. M. W., Remis, R. F., Stalpers, L. J.A., Westerveld, He., Nederveen, A. J., van den Berg, C. A.T., and Crezee, J., 2016, "Hyperthermia Treatment Planning for Cervical Cancer Patients Based on Electrical Conductivity Tissue Properties Acquired In Vivo With EPT at 3 T MRI," Int. J. Hyperthermia, **32**(5), pp. 558–568.
[172] Katscher, U., Voigt, T., Findeklee, C., Vernickel, P., Nehrke, K., and Dossel, O., 2009, "Determination of Electric Conductivity and Local SAR via B1 Mapping," IEEE Trans. Med. Imaging, **28**(9), pp. 1365–1374.
[173] Zhang, X., Schmitter, S., Van de Moortele, P., Liu, J., and He, B., 2013, "From Complex B(1) Mapping to Local SAR Estimation for Human Brain MR Imaging Using Multi-Channel Transceiver Coil at 7 T," IEEE Trans. Med. Imaging, **32**(6), pp. 1058–1067.
[174] Wang, Y., Van de Moortele, P.-F., and He, B., 2019, "Automated Gradient-Based Electrical Properties Tomography in the Human Brain Using 7 Tesla MRI Automated Gradient-Based Electrical Properties Tomography in the Human Brain Using 7 Tesla MRI," Magn. Reson. Imaging, **63**, pp. 258–266.
[175] Hancu, I., Roberts, J. C., Bulumulla, S., and Lee, S.-K., 2015, "On Conductivity, Permittivity, Apparent Diffusion Coefficient, and Their Usefulness as Cancer Markers at MRI Frequencies," Magn. Reson. Med., **73**(5), pp. 2025–2029.
[176] Colton, D., and Kress, R., 1998, *Inverse Acoustic and Electromagnetic Scattering Theory*, Springer-Verlag, Berlin, Germany.
[177] Bertero, M., and Boccacci, P., 1998, *Introduction to Inverse Problems in Imaging*, Institute of Physics, Bristol, UK.
[178] Bevacqua, M. T., Bellizzi, G. G., Isernia, T., and Crocco, L., 2019, "A Method for Effective Permittivity and Conductivity Mapping of Biological Scenarios via Segmented Contrast Source Inversion," Prog. Electromagn. Res., **164**, pp. 1–15.
[179] Bevacqua, M. T., Bellizzi, G. G, Crocco, L., and Isernia, T., 2019, "A Method for Quantitative Imaging of Electrical Properties of Human Tissues From Only Amplitude Electromagnetic Data," Inverse Prob., **35**(2), pp. 025006IP.
[180] Golnabi, A. H., Meaney, P. M., and Paulsen, K. D., 2016, "3D Microwave Tomography of the Breast Using Prior Anatomical Information," Med. Phys., **43**(4), pp. 1933–1944.
[181] Meaney, P. M., Golnabi, A. H., Epstein, N. R., Geimer, S. D., Fanning, M. W., Weaver, J. B., and Paulsen, K. D. 2013, "Integration of Microwave Tomography With Magnetic Resonance for Improved Breast Imaging," Med. Phys., **40**(10).
[182] Neira, K. M., Van Veen, B. D., and Hagness, S. C., 2017, "High-Resolution Microwave Breast Imaging Using a 3-D Inverse Scattering Algorithm With a Variable-Strength Spatial Prior Constraint," IEEE Trans. Antennas Propag., **65**(11), pp. 6002–6014.
[183] Rahimov, A., Litman, A., and Ferrand, G., 2017, "MRI-based Electric Properties Tomography With a Quasi-Newton Approach," Inverse Prob., **33**(10), p. 105004.
[184] Isernia, T., Pascazio, V., and Pierri, R., 2001, "On the Local Minima in a Tomographic Imaging Technique," IEEE Trans. Geosci. Remote Sens., **39**(7), pp. 1596–1607.
[185] Winters, D. W., Shea, J. D., Kosmas, P., Van Veen, B. D., and Hagness, S. C., 2009, "Three-Dimensional Microwave Breast Imaging: Dispersive Dielectric Properties Estimation Using Patient-Specific Basis Functions," IEEE Trans. Med. Imaging, **28**(7), pp. 969–981.
[186] Scapaticci, R., Kosmas, P., and Crocco, L., 2015, "Wavelet-Based Regularization for Robust Microwave Imaging in Medical Applications," IEEE Trans. Biomed. Eng., **62**(4), pp. 1195–1202.
[187] Catapano, L., Di Donato, L., Crocco, L., Bucci, O. M., Morabito, A. F., Isernia, T., and Massa, R., 2009, "On Quantitative Microwave Tomography of Female Breast," Prog. Electromagn. Res., **97**, pp. 75–93.
[188] Shea, J. D., Kosmas, P., Hagness, S. C., and Van Veen, B. D., 2010, "Three-Dimensional Microwave Imaging of Realistic Numerical Breast Phantoms via a Multiple-Frequency Inverse Scattering Techniques," Med. Phys., **37**(8), pp. 4210–4226.
[189] Fedeli, A., Maffongelli, M., Monleone, R., Pagnamenta, C., Pastorino, M., Poretti, S., Randazzo, A., and Salvadè, A., 2018, "A Tomograph Prototype for Quantitative Microwave Imaging: Preliminary Experimental Results," J. Imaging, **4**(12), pp. 1–9.
[190] Hopfer, M., Planas, R., Hamidipour, A., Henriksson, T., and Semenov, S., 2017, "Electromagnetic Tomography for Detection, Differentiation, and Monitoring of Brain Stroke: A Virtual Data and Human Head Phantom Study," IEEE Antennas Propag. Mag., **59**(5), pp. 86–89.
[191] Mojabi, P., and LoVetri, J., 2009, "Microwave Biomedical Imaging Using the Multiplicative Regularized Gauss–Newton Inversion," IEEE Antennas Wirel. Propag. Lett., **8**, pp. 645–648.
[192] Alqadami, A., Zamani, A., Trakic, A., and Abbosh, A., 2021, "Flexible Electromagnetic cap for Three-Dimensional Electromagnetic Head Imaging," IEEE Trans. Biomed. Eng., **68**(9), pp. 2880–2891.
[193] Meaney, P. M., Fanning, M. W., Raynolds, T., Fox, C. J., Fang, Q., Kogel, C. A., Poplack, S. P., and Paulsen, K. D., 2007, "Initial Clinical Experience with Microwave Breast Imaging in Women With Normal Mammography," Acad. Radiol., **14**(2), pp. 207–218.
[194] Norouzzadeh, E., Chamaani, S., Moll, J., Kexel, C., Nguyen, D. H., Hübner, F., Bazrafshan, B., Vogl, T. J., and Krozer, V., 2020, "Numerical and Experimental Analysis of a Transmission-Based Breast Imaging System: A Study of Application to Patients," Int. J. Microwave Wireless Technolog., **12**(6), pp. 469–476.
[195] Fear, E. C., Bourqui, J., Curtis, C., Mew, D., Docktor, B., and Romano, C., 2013, "Microwave Breast Imaging With a Monostatic Radar-Based System: A Study of Application to Patients," IEEE Trans. Microwave Theory Tech., **61**(5), pp. 2119–2128.
[196] Preece, A. W., Craddock, I., Shere, M., Jones, L., and Winton, H. L., 2016, "MARIA M4: Clinical Evaluation of a Prototype Ultrawideband Radar Scanner for Breast Cancer Detection," J. Med. Imaging, **3**(3), pp. 033502.
[197] O'Rourke, A. P., Lazebnik, M., Bertram, J. M., Converse, M. C., Hagness, S. C., Webster, J. G., and Mahvi, D. M., 2007, "Dielectric Properties of Human Normal, Malignant and Cirrhotic Liver Tissue: In-Vivo and Ex-Vivo Measurements From 0.5 to 20 GHz Using a Precision Open-Ended Coaxial Probe," Phys. Med. Biol., **52**(15), pp. 4707–4719.
[198] Salahuddin, S., La Gioia, A., Elahi, M. A., Porter, E., O'Halloran, M., and Shahzad, A., 2017, "Comparison of In-Vivo and Ex-Vivo Dielectric Properties of Biological Tissues," Proceedings of the International Conference on Electromagnetics in Advanced Applications, Verona, Italy, Sept. 11–15, pp. 582–585.
[199] Haemmerich, D., Ozkan, O. R., Tsai, J. -Z., Staelin, S. T., Tungjitkusolmun, S., Mahvi, D. M., and Webster, J. G., 2002, "Changes in Electrical Resistivity of Swine Liver After Occlusion and Postmortem," Med. Biol. Eng. Comput., **40**(1), pp. 29–33.
[200] Gabriel, C., and Peyman, A., 2018, "Variation with Age; Chapter 69," *Dielectric Properties of Biological Tissues, Conn's Handbook of Models for Human Aging*, 2nd ed., J. L. Ram, and P. Michael Conn, eds., Academic Press, London, UK, pp. 939–952.
[201] Meaney, P. M., Zhou, T., Golnabi, A., Attardo, E. A., and Paulsen, K. D., 2012, "Bone Dielectric Property Variation as a Function of Mineralization at Microwave Frequencies," Int. J. Biomed. Imaging, **2012**, pp. 1–10.
[202] Keysight Technologies, 2022, "N1501A Dielectric Probe Kit," Keysight Technologies, https://www.keysight.com/us/en/assets/7018-04631/technical-overviews/5992-0264.pdf.
[203] Gregory, A. P., and Clarke, R. N., 2009, "Tables of the Complex Permittivity of Dielectric Reference Liquids at Frequencies up to 5 GHz," National Physical Laboratory.
[204] Peyman, A., Gabriel, C., and Grant, E. H., 2007, "Complex Permittivity of Sodium Chloride Solutions at Microwave Frequencies," Bioelectromagnetics, **28**(4), pp. 264–274.
[205] Kilian, D., Kilian, W., Troia, A., Nguyen, T.-D., Ittermann, B., Zilberti, L., and Gelinsky, M., 2022, "3D Extrusion Printing of Biphasic Anthropomorphic Brain Phantoms Mimicking MR Relaxation Times Based on Alginate-Agarose-Carrageenan Blends," ACS Appl. Mater. Interfaces, **14**(43), pp. 48397–48415.
[206] Meerbothe, T. G., Florczak, S., Stijnman, P. R., van den Berg, C. A., Levato, R., and Mandija, S., 2022, "A Semi-Realistic and Reusable 3D Printed Brain Phantom for MR-Based Electrical Properties Tomography," Proc. Intl. Soc. Mag. Reson. Med, **31**, pp. 2921.
[207] Wilkinson, M. D., Dumontier, M., Aalbersberg, I. J., Appleton, G., Axton, M., Baak, A., Blomberg, N., et al., 2016, "The FAIR Guiding Principles for Scientific Data Management and Stewardship," Sci. Data, **3**(1), pp. 160018.
[208] Brazma, A., Hingamp, P., Quackenbush, J., Sherlock, G., Spellman, P., Stoeckert, C., Aach, J., et al., 2001, "Minimum Information About a Microarray Experiment (MIAME)-Toward Standards for Microarray Data," Nat. Genet., **29**(4), pp. 365–371.